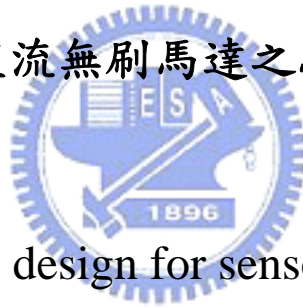


國立交通大學

機械工程學系

碩士論文

無感測直流無刷馬達之驅動電路設計



Driver circuits design for sensorless BLDC motor

研究生：徐舫強

指導教授：成維華 教授

中華民國九十七年七月

無感測直流無刷馬達之驅動電路設計

Driver circuits design for sensorless BLDC motor

研究生：徐舫強

Student : Po-Ch'iang Hsu

指導教授：成維華

Advisor : Wei-Hua Chieng

國立交通大學

機械工程學系

碩士論文



A Thesis
Submitted to Institute of Mechanical Engineering
College of Engineering

National Chiao Tung University

in partial Fulfillment of the Requirements

for the Degree of

Master

In

Mechanical Engineering

July 2008

Hsinchu, Taiwan, Republic of China

中華民國九十七年七月

無感測直流無刷馬達之驅動電路設計

研究生：徐 舶 強

指導教授：成 維 華 博士

國立交通大學機械工程學系

摘要

直流無刷馬達在現今工業裡扮演著重要的角色，主要是因為據有高效率、高轉速以及高扭力等優點。一般直流馬達運轉時，需要霍爾原件來偵測轉子的位置做換相的機制，但使用霍爾原件除了成本提高之外，也容易受環境溫度所限制。若能夠不使用霍爾原件來做換相的機制，就可以使成本降低，固有許多無感測的方法被提出。

本論文設計一無感測直流無刷馬達驅動器，有別於一般感測反電動勢零交越電路，此驅動器只需要量測非激發端的電壓就可以估測轉子位置做換相的動作。論文最後比較有感測與無感測驅動之差異，發現在某些特定的情況下，無感測驅動是可以取代有感測驅動。

Driver Circuits design for sensorless BLDC motor

Student : Po-Ch'iang Hsu

Advisor : Dr. Wei-Hua Chieng

Institute of Mechanical Engineering

National Chiao Tung University

Abstract

The BLDC motors are play important roles in this industry. It is because that the BLDC motors possess some advantages such as high efficiency, high speed and high torque. In general, the BLDC motors work need hall sensor to detect the rotor position in order to commute. Nevertheless, use hall sensors not only increase cost but also restricted to surrounding temperature. If the motor commute without hall sensors, we can cost down. Therefore, many sensorless methods are proposed.

The thesis designs a driver for a sensorless BLDC motor. Differ from general drivers, my driver estimates rotor position according to unexcited phase voltage and then commute without any Back-EMF detection circuits. In the end of the thesis, I compare the differences with sensor control and sensorless control. In the certain condition, the sensorless control could replace with sensor control.

誌 謝

首先誠摯的感謝成維華教授以及鄭時龍博士，在我兩年的碩士生活中不斷的鞭策我、磨練我，兩位老師做學問嚴謹的態度是這兩年來使我不斷進步的原動力。在此，再一次的感謝兩位老師的細心指導。

終於...畢業了! 想要感謝的人...太多了! 感謝黑人的“吃宵”; 感謝葛雷的“少囉嗦”; 感謝小色狼的“鹹豬手”; 感謝曹兄的“開戰了”; 感謝磊哥的“駕!”; 感謝羊豪的“謝謝你”; 感謝文彬“打死一頭牛”; 感謝小賴的“第一牙套”; 感謝學弟們一聲聲的“強哥”。感謝沒感謝到的人，因為你們點點滴滴的蝴蝶效應才能造就了今日的我，我會把你們放在心裡由衷的感謝。

求學 18 個年頭，終於要在這裡暫時先告一個段落。爸媽謝謝你們無怨無悔的付出與支持，讓我可以無後顧之憂的去追求理想。阿珩、阿 Du，妳弟很爭氣地拿到了碩士學位，希望妳們都能平安幸福。最後謝謝小方一路上的鼓勵，這些日子因為有妳的相伴，讓我擁有一段難忘的回憶。

最最最要感謝的是強哥...“Congratulations! You got it.”

目 錄

摘要	i
Abstract	ii
誌 謝	iii
目 錄	iv
List of Figures	vi
List of tables	viii
Chapter 1 Introduction.....	1
1.1 Research motive	1
1.2 Thesis Organization	1
Chapter 2 Basic Concepts of BLDC Motors.....	3
2.1 Characteristics of BLDC Motors.....	3
2.2 Mathematical Modeling of BLDC Motor	4
2.3 Typical Commutation Principle	6
2.4 Speed control analysis.....	7
2.5 Back-EMF based position estimation method	9
Chapter 3 Sensorless control of a BLDC motor.....	14
3.1 Back-EMF Waveforms	14
3.2 Procedures of sensorless control.....	15
3.3 Sensorless Feedback control	17
3.3.1 Synchronous Mode	19
3.3.2 Accelerate Mode.....	19
3.3.3 Speed Locked Mode.....	20

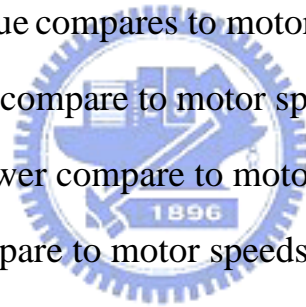
Chapter 4 Experiments and comparisons	22
4.1 A brief introduction of MCU	22
4.2 Sensorless BLDC driver circuits	23
4.3 Experiment results	24
Chapter 5 Conclusion	26
Reference	27



List of Figures

Fig 2.1 The configuration of BLDC motors.....	31
Fig 2.2 Equivalent modeling for a BLDC Motor.....	31
Fig 2.3 Schematic of the inverter and equivalent modeling for a BLDC motor	32
Fig 2.4 Ideal BEMF and phase current waveform of a BLDC motor	32
Fig 2.5 The procedure of six-step drive	33
Fig 2.6 Phase voltage in commutation	34
Fig 2.7 A BLDC motor equal circuits	34
Fig 2.8 Hall-sensor	35
Fig 2.9 System framework of typical Hall-sensors commutation control	35
Fig 2.10 Detection of switching point P from the crossing of the neutral voltage and terminal voltage.	36
Fig 3.1 3-Phases voltage	36
Fig 3.2 Sensorless BLDC state diagram	36
Fig 3.3 Motor current compare to duty cycle.....	37
Fig 3.4 System framework of sensorless control	37
Fig 3.5 four slots in the unexcited phase.....	38
Fig 3.6 The relationship between PWM and commutation time without loading.....	38
Fig 3.7 Synchronous mode function block of MCU.....	39
Fig 3.8 Accelerate mode function block of MCU	39
Fig 3.9 Speed locked mode function block of MCU	40
Fig 3.10 Flow chart of feedback control	40

Fig 4.1 C8051F340 target board	41
Fig 4.2 C8051F340 block diagram.....	41
Fig 4.3 The sensorless BLDC driver circuits	42
Fig 4.4 Display circuits	42
Fig 4.5 MOSFET driver circuits	43
Fig 4.6 Detect current circuits	43
Fig 4.7 Lowpass filter circuits for filter noise.....	44
Fig 4.8 A front view of driver circuits.....	45
Fig 4.9 A back view of driver circuits	45
Fig 4.10 Experiment instrument.....	46
Fig 4.11 Maximum torque compares to motor speeds	47
Fig 4.12 Current ranges compare to motor speeds.....	47
Fig 4.13 Mechanical power compare to motor speeds	48
Fig 4.14 Efficiency compare to motor speeds.....	48



List of tables

Table 2.1 The schedule of 120° six-step square commutation.....	29
Table 3.1 Back-EMF waveform control.....	30



Chapter 1 Introduction

1.1 Research motive

Nowadays, there are many kinds of serve motors apply to industry. Among them, the brushless direct current motors (BLDC motor) become more and more attractive for many industrial applications, such as compressors, electrical vehicles and DVD players etc. comparing with other motors, BLDC motors possess some advantages such as high torque, high power density and high efficiency. Unlike conventional DC motors, the BLDC motor commutate without a brush. Therefore, they have no problems in abrasions and sparkles from mechanical contact.

In general, the BLDC motor often needs the sensor to detect the rotor position in order to get the correct commutation time. With a sensor, it increases not only volume but also the cost. Furthermore, it could not work in the higher temperature environment. Therefore, many people start to investigate the methods of sensorless control.

1.2 Thesis Organization

The thesis is divided in five chapters. In chapter 1, explain why a BLDC motor is so popular in industry. In view of above mention, more and more people start to improve the BLDC control in order to cost

down and apply widely.

In chapter 2, some characteristics of BLDC motors will be introduced. Besides, mathematical modeling [1], commutation principle and speed control analysis of BLDC motors are also illustrated. In the end of this chapter, the most important part which is Back-EMF based position estimation method [2, 3, 4] will be illustrated.

The chapter 3 is the core of this thesis. How to interpret the Back-EMF waveform? What procedures will be taken in the sensorless control? How does the closed loop control work? Those questions will explain in this chapter.

In chapter 4, I will introduce my experiment instrument, controller and experiment results. Beside of above mentions, I also introduce the driver circuits in detail.

Chapter 5 is my conclusion. According to the experiments, I bring up some proportions about sensorless control.

Chapter 2 Basic Concepts of BLDC Motors

A brushless DC (BLDC) motor is a rotating electric machine where the stator is a class three-phase stator like that of an induction motor and the rotor has surface-mounted permanent magnet. In this chapter, the basic configuration and the characteristics of BLDC motors will be described in Section 2.1. Then the mathematical modeling will be represented in Section 2.2. Furthermore, a BLDC motor requires an inverter and a position sensor to perform “commutation” because a permanent magnet synchronous motor takes the place of DC motor with brushes and commutators. Thus, the detail commutation and excited procedure will be illustrated in Section 2.3. The Speed control analysis is spread out in section 2.4. In section 2.5, introduce the sensorless BLDC motor and its commutation methods.

2.1 Characteristics of BLDC Motors

In general, a BLDC motor consists of a permanent magnet synchronous motor that converts electrical energy to mechanical energy. The basic configuration of BLDC motors are shown in Fig2.1. In this figure, it's clear to see the BLDC motor which consists of permanent magnets is on the rotor and the armature is on the stator. On the other hand, A BLDC motor comes in 2-Phase, 3-phase and 4-phase configuration.

Corresponding to its type, the stator has the same numbers of windings. Furthermore the Hall elements are installed inside the stator to detect the rotor position. Since the 3-phase BLDC motors have three windings which are distributed with 120° in electrical degree apart to each other, the driver structure including the six-step inverters using PWM signals. Thus, the principle of switching is based on electrical angular position information, which is decoded by three Hall-effect sensors.

2.2 Mathematical Modeling of BLDC Motor

In general, a BLDC motor has a permanent-magnet rotor and its stator windings are wound to generate the back electromotive force (Back-EMF). The dynamic equations of BLDC motors with Y-connected stator windings are shown in Fig2.2.

We can use Kirchhoff's law and Newton's law to formulate 3-phase BLDC electromagnetic equation and dynamic equation [5], which express as

Electromagnetic equation:

$$\begin{bmatrix} V_a \\ V_b \\ V_c \end{bmatrix} = \begin{bmatrix} R & 0 & 0 \\ 0 & R & 0 \\ 0 & 0 & R \end{bmatrix} \begin{bmatrix} i_a \\ i_b \\ i_c \end{bmatrix} + \begin{bmatrix} L_p & -M & -M \\ -M & L_p & -M \\ -M & -M & L_p \end{bmatrix} \begin{bmatrix} \dot{i}_a \\ \dot{i}_b \\ \dot{i}_c \end{bmatrix} + \begin{bmatrix} e_a \\ e_b \\ e_c \end{bmatrix} \quad (2-1)$$

Among, the back electromotive force (Back-EMF) express as

$$\begin{bmatrix} e_a \\ e_b \\ e_c \end{bmatrix} = \frac{2\omega_r K_e}{P} \begin{bmatrix} \sin(\theta_e) \\ \sin(\theta_e - \frac{2\pi}{3}) \\ \sin(\theta_e + \frac{2\pi}{3}) \end{bmatrix} \quad (2-2)$$

Dynamic equation:

$$\begin{aligned} T_e &= K_t(i_a - \frac{i_b}{2} - \frac{i_c}{2})\sin(\theta_e) + \frac{\sqrt{3}}{2}(i_c - i_b)\cos(\theta_e) \\ &= \frac{2J}{P}\dot{\omega}_r + \frac{2B_m}{P}\omega_r + T_L \end{aligned} \quad (2-3)$$

V_a, V_b, V_c : a, b, and c phase voltages

i_a, i_b, i_c : a, b, and c phase currents

e_a, e_b, e_c : a, b, and c phase back electromotive force

L_p : self-inductance of a, b and c phase

M : mutual inductance between any two phase

R : stator resistance

ω_r : rotor speed

θ_e : angle between stator phase A and rotor

K_e : Back-EMF constant

P : number of pole pairs

T_e : electric torque

K_t : torque constant

T_L : load torque

J : moment of inertia

B_m : damping constant

2.3 Typical Commutation Principle

The model of the three phases Y-connected BLDC motor consists of winding resistances, winding inductances, and Back-EMF voltage sources. The inverter circuits and the equivalent model are shown in Fig 2.3. If the rotor rotates, the outer stator's magnetic field must be change in according to rotor's position. We input current in the winding of stator to change magnetic field, and then generate torque. As the result of the stator is fixed, the reactive force pushes inner rotor and then the BLDC rotates. The typical commutation for a BLDC motor is accomplished by controlling the six inverter switches according to the six-step sequences to produce the phase current waveforms as shown in Fig 2.4. Ideally, the currents are in rectangular shapes, and the stator inductance voltage may be neglected. Thus, the sequence of the conducting phase will be shown in Table 2.1. The detail commutation and excited procedure are illustrated with a two

poles and six slots BLDC motor as shown in Fig 2.5

Actually, the phase voltage is unlike Fig 2.4. As a result of motor is inductive load, the current which passes the winding can't shut down as the switch is right OFF. Instead, the current will decrease stage by stage. This phenomenon results in that the current passes the Free-Wheeling diode. If the current passes high-arm Free-Wheeling diode, the phase is down sharply instantly. Contrary, the phase voltage is up sharply as the current passes low-arm Free-Wheeling diode. The detail explanation is shown in Fig 2.6.



2.4 Speed control analysis

Fig 2.7 is the BLDC equal circuits. The voltage equation can be derived from the circuits as

$$V_s(PWM) = V_{CE(sat)} + IR_a + E$$

$$I = \frac{V_s(PWM) - V_{CE(sat)} - E}{R_a} \quad (2-4)$$

$V_s(PWM)$: Average effective voltage

$V_{CE(sat)}$: BJT's conduct Voltages between collection and emitter

I : Equal total current

R_a : Equal total resistance

E : Back-EMF

The term V_{CE} is so small that can be ignored. So the equation can be rewritten as

$$\begin{aligned} V_s(PWM) &= IR_a + E \\ I &= \frac{V_s(PWM) - E}{R_a} \end{aligned} \quad (2-5)$$

Beside the voltage equation, the torque equation and Back-EMF equation are also need in order to analyze speed control. The torque equation and Back-EMF equation are represented individually as

$$T = K_t \cdot I \quad (2-6)$$

$$E = K_e \cdot \omega_r \quad (2-7)$$

According equations (2-5), (2-6) and (2-7), we can analyze situations when BLDC motors are in acceleration and deceleration. In the case of acceleration, PWM increases results in the average effective voltage increases, according to equation (2-5), the current I also increases, according equation (2-6), the induced torque of stator $T_{induced}$ increases follows the current I increases. When the $T_{induced}$ is larger than the loading torque T_{load} , the motor's speed increases. According to equation (2-7), the Back-EMF increases when the motor's speed increases. The result makes the current I decreases. When the current I is down, the $T_{induced}$ decreases until $T_{induced}$ equals to T_{load} . Therefore, the speed is not only accelerated but also stable. In the other case of deceleration, the analysis is opposite, PWM decreases results in the average effective

voltage decreases, according to equation (2-5), the current I also decreases, according equation (2-6), the induced torque of stator $T_{induced}$ decreases follow the current I decreases. When the $T_{induced}$ is smaller than the loading torque T_{load} , the motor's speed decreases. According to equation (2-7), the Back-EMF decreases when the motor's speed decreases. The result makes the current I increase. When the current I is up, the $T_{induced}$ increases until $T_{induced}$ equals to T_{load} . Base on the analysis, the speed control can easily implement.

2.5 Back-EMF based position estimation method

Since BLDC Motors use permanent magnets for excitation, rotor position sensors are needed to perform electrical commutation. Commonly, three Hall-effect sensors installed inside the BLDC motor are used to detect rotor position. The Hall sensor is shown in Fig 2.8. The theorem is that add magnetic field on the semiconductor which current passed and then the Hall voltage be shown in the direction which orthogonal to the directions of passed current and magnetic field. The voltages change with rotor's position. According to Hall voltage, commutation time could be decided. The system schematic of typical Hall commutation is shown in Fig 2.9, and the Hall voltage can be expressed as

$$V_H = K \cdot \frac{I_c}{d} \cdot B \quad (2-8)$$

K : Hall constant

I_c : Passed current

d : Thickness of element

B : Magnetic field

However, the rotor position sensors present several drawbacks from the viewpoint of total system cost, size, and reliability. Therefore, many investigators have paid more and more attentions to sensorless control without any Hall sensors and proposed many sensorless-related technologies. To follow, I will introduce the technique that estimate the rotor's position depend on measuring back-EMF [6, 7].

The rotor position is obtained directly by measurement of the Back-EMF induced in the stator windings. In the basic operation of a BLDC motor, only two phases are energized at any instant and the other phase is unexcited. Therefore, the unexcited phase contains the Back-EMF information that can be used to derive the commutation time. The Back-EMF zero-crossing method is employed to determine the switching sequence by detecting the instant when the Back-EMF crosses zero point in the unexcited phase.

Consider the inverter circuits are connected to a BLDC motor with Y-connected stator windings, as shown in Fig 2.2, three terminal voltages v_a , v_b and v_c can be derived as

$$v_a = v_{an} + v_n = R_s i_a + L_s \frac{di_a}{dt} + e_a + v_n \quad (2-9)$$

$$v_b = v_{bn} + v_n = R_s i_b + L_s \frac{di_b}{dt} + e_b + v_n \quad (2-10)$$

$$v_c = v_{cn} + v_n = R_s i_c + L_s \frac{di_c}{dt} + e_c + v_n \quad (2-11)$$

Where v_n is the neural voltage, v_{an} , v_{bn} and v_{cn} are the phase voltages with respect to the negative DC bus. i_a , i_b and i_c represent the phase currents, and e_a , e_b and e_c are the Back-EMF voltages generated in the three phases. In order to describe the zero-crossing method, assumes S_1 and S_5 turn on, the terminal voltages v_a , v_b and v_c become

$$v_a = V_{dc} \quad (2-12)$$

$$v_b = 0 \quad (2-13)$$

$$v_c = e_c + v_n \quad (2-14)$$

Ideally, it is assumed that the current applied to the winding is rectangular-shaped and the stator inductance voltage drop is negligible. The

relationship of the line-to-line current i_{ab} and corresponding phase currents i_a and i_b can be shown as

$$i_{ab} = i_a = -i_b = \frac{V_{dc} - (e_a - e_b)}{2R_s} \quad (2-15)$$

According to (3-8), (3-9), (3-10), and (3-11), the terminal voltage of phase C can be derived as

$$v_c = e_c + v_n = e_c + \frac{V_{dc} - e_a - e_b}{2} \quad (2-16)$$

Since the difference of 120° electrical degree in Back-EMF voltages between with any two phases, there is an instant that $e_c = 0$ and $e_a = -e_b$. Then

$$v_c = v_n = \frac{V_{dc}}{2} \quad (2-17)$$

Hence, the Back-EMF zero-crossing position of e_c is independent of the load current. The terminal voltage v_a and v_b have the same relationship as v_c and v_n when phase a or b is unexcited. After detecting the Back-EMF zero-crossing position of the unexcited phase, it is well know that the input signal of the unexcited phase should be given with 90°

electrical degree delay to get the maximum torque, as shown in Fig 2.10. The method can be realized by using voltage comparators and low-pass filters. However, the modulation noise is eliminated by using the low-pass filter, this causes a phase delay varies with the frequency of the excited signal for the desired rotor speed. Besides, the BEMF voltage is zero at standstill and is proportional to the rotor speed. This method cannot be used at startup situation and works poorly at low-speed operation.



Chapter 3 Sensorless control of a BLDC motor

This chapter introduces the sensorless control of a BLDC motor. In section 3.1, illustrate how to interpret the different Back-EMF waveforms. Then, the sensorless control procedures will be introduced in detail in section 3.2 and section 3.3.

3.1 Back-EMF Waveforms

Most sensorless BLDC control system use the Back-EMF zero crossing time as a control variable for a phase locked loop as shown in Fig 3.1. Instead of using the Back-EMF zero-crossing time, this thesis design measures the Back-EMF voltage at middle of the commutation period using the ADC and uses the voltage measurement to control the commutation. This method provides higher resolution and always provides a robust feedback signal even as the motor approaches a stall condition.

The Back-EMF voltage for three different cases is shown in Table 3.1. If the voltage and speed are just right the voltage ramp will be centered within the commutation period and the midpoint voltage will measure half of the supply rail. If the voltage is too low or the speed is

too fast the voltage ramp will be shifted up and to the right. If the voltage is too high or the speed is too slow, the voltage ramp will be shifted down and to the left. The feedback loop should work to keep the mid-point voltage at mid-rail.

Now consider what happens when commutation is too fast. When commutation occurs early the Back-EMF has not reached peak resulting in more motor current and a greater rate of acceleration to the next phase but it will arrive there too late. The motor tries to keep up with the commutation but at the expense of excessive current. If the commutation arrives so early that the motor could not accelerate fast enough to catch the next commutation, lock is lost and the motor spins down. This happens abruptly not very far from the ideal rate.

Consider another case what happens when commutation is too slow for applied voltage, the Back-EMF will be too low resulting in more motor current. The motor will react by accelerating to next phase position then slow down waiting for the next commutation. In the extreme case the motor will snap to each position like a stepper motor until the next commutation occurs. Since the motor is able to accelerate faster than the ideal can be tolerate without losing lock but at the expense of excessive current.

3.2 Procedures of sensorless control

Generally, there are four procedures in sensorless control. They individually are “STOP”, “ALIGE”, “START” and “RUN” as show in Fig 3.2. In the procedure of “STOP”, the state means the motor is stopped and the PWM duty cycle is turned off. The others will be illustrated in the following section.

The sensorless BLDC motors rotate depend on fixed commutation sequences. Therefore, we must know the initial position of a rotor before rotating. In the procedure of “ALIGN”, we excite the specific stator in order to compel the rotor aligned. The alignment state consists of two stages – the alignment ramp and the alignment delay. During the alignment ramp, one of the motor windings is excited by PWMing the top of the one phase and the bottom of another phase. The PWM duty cycle is initially at zero percent and is ramped up to 50% plus the starting boost voltage. The voltage is increased using a linear ramp with a fixed delay time between voltage increments. The current in the motor winding will depend on the motor inductance and winding resistance. For duty cycles below 50% the current will be discontinuous. The current will increase while the transistors are on and decrease to zero after the transistors turn off as shown in Fig 3.3. For duty cycles above 50% the current will be continuous. Usually a higher current is desired for alignment. Above 50%, a small change in duty cycle will result in a much large change in average DC current. The starting boost voltage is typically a very small number. The second part of the alignment phase consists of a simple delay. The alignment delay time should be long

enough to allow the motor to align to the excited pole position. Finding the optimal delay time requires some experimentation.

In the second procedure “ALIGN”, we get the position of a rotor. Now, we can rotate the rotor depend on fixed commutation procedures. Remember! Our goal is that motor commutates automatic depend on Back-EMF. Look back the equation (2-2), the Back-EMF is direct ratio to motor speed. The Back-EMF is too small to use in the closed loop control at lower speed. Therefore, we must accelerate the motor to induce enough Back-EMF. In the third procedure “START”, the motor is driven like a stepper motor. The motor is commutated at first very slowly and then velocity is increased linearly using a linear velocity ramp table. The voltage is also increased in proportion to the velocity with additional boost voltage to keep the current at a constant value. By the way, duty cycle must open more if the motor have preload. This can ensure the motor rotate well instead of stall. At the same time, be careful of your current when adding more PWM duty cycle. Over current may burn the driver or the motor. In my control, I compel the motor to accelerate approximately 1000 rpm. Then, the control can enter next procedure ”RUN”. About the state of ”RUN” will be introduced in detail in the next section.

3.3 Sensorless Feedback control

This section is the core of the thesis. If the motor passes through the procedures “ALIGN” and “START”, the motor enters the final procedure “RUN”. In other word, procedure “RUN” is feedback control. In this procedure, I design three modes in the feedback control. They are individually Synchronous Mode, Accelerate Mode and Speed Locked Mode. Fig 3.4 is the system framework of the sensorless feedback control. Microprocessor control unit (MCU) gets unexcited terminal voltage to determine the Back-EMF waveforms. In practice, I divide one commutation time into four slots as shown in Fig 3.5. Every slot is an interruption. A commutation time has four interruptions. In the first interruption, MCU just commands to commutate and ADC (analog voltage converts into digital number) the voltage which detects current on the driver circuits. If the current is over than the safe range, take the sequence in the procedure “STOP”. In the second and fourth interruptions, MCU ADC the Back-EMF individually to determinate the motor is stall or not. If the differential voltages of second ADC and fourth ADC are less than certain value, the motor maybe stall. In the opposite, the motor is stable. The third interrupt is used to detect how differential voltages between the Back-EMF and zero-crossing voltage. Modulate the commutation time according the differential voltages. Fig 3.6 is the figure that describes the relationship between PWM and commutation time without loading. In the figure, we can find that much commutation time varied just results in small speed varied at lower speed. But at higher speed, small commutation time varied can result in much

speed varied. The phenomenon tells us that we must take different controls at different speeds. At low speed, we make sensitive PI control to compensate our system. At high speed, we make sluggish PI control to compensate our system. A better PI control must have more experiments.

3.3.1 Synchronous Mode

When the procedure “START” transfers to the procedure “RUN”, the first station of the procedure “RUN” is into Synchronous Mode. In the procedure “START”, the PWM duty cycle and commutation time are varied depend on the Table. With different preload and temperature of the motor, the Back-EMF waveforms are also different. This will result in asynchronous between phase current and Back-EMF. In Synchronous mode, our goal is make them be synchronous. First, lock the PWM at 131 (8 bits) which been set in the end of the procedure “START”. Then, modulate the commutation time according to the voltages which been ADC in third interrupt. The Fig 3.7 is the Synchronous Mode function of the MCU. When the synchronous delay time is matured, the control sequence will automatic jump into Accelerate Mode.

3.3.2 Accelerate Mode

This mode is avoid to stall when the BLDC motor decelerate or

accelerate rapidly. The function blocks are shown in the Fig 3.8. Modulate the variable resistance as the speed-command. Then, the speed-command subtract the estimated speed, we can get speed error. Throw the speed error into Speed controller. In the Speed controller, a controller modulates the PWM step by step instead of immediately. On the other hand, the commutation PI control also calculates the compensated commutation time by the error voltage which ADC in third interrupt. Through recalculated commutation time, we can estimate the motor speed for calculating the next speed error.

3.3.3 Speed Locked Mode

This mode is very similar to Accelerate Mode. The function blocks are shown in the Fig 3.9. The difference is speed locked or not. In the Accelerate Mode, the speed can modulate depend on speed-command. But in the Speed locked Mode, the speed-command is fixed. In other words, if the speed-command is changed, the procedure jumps into Accelerate Mode automatically. When the speed-command is stand in a space, the procedure jumps into Speed locked Mode automatically. Besides, in the Speed Locked Mode, the speed error is thrown into speed PI controller rather than the controller which the Accelerate Mode uses. Therefore, the system will have more sensitive compensation. Compared with Accelerate Mode, the motor have larger torque in the Speed Locked Mode.

The Fig 3.10 is the flow char of the feedback control. All feedback control is designed in the interruption of Timer2. Every interruption takes five microseconds. About detail hardware and experiments will be introduced in the next chapter.

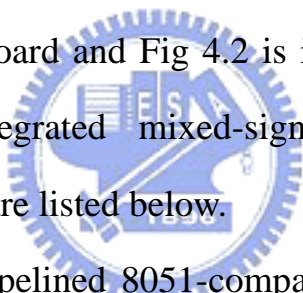


Chapter 4 Experiments and comparisons

In this chapter, I implement the sensorless control depend on the methods which been taken before. Then, I test my sensorless BLDC motor in T_{\max} - N curve and efficiency. Besides, I also introduce the MCU and the driver circuits.

4.1 A brief introduction of MCU

In the thesis, I use the **Silicon C8051F340DK** to be my controller. Fig 4.1 is its target board and Fig 4.2 is its block diagram. C8051F340 device is fully integrated mixed-signal system-on-a-chip MCUs. Highlighted features are listed below.

- 
- a. High-speed pipelined 8051-compatible microcontroller core (up to 48 MIPS)
 - b. In-system, full-speed, non-intrusive debug interface (on-chip)
 - c. Universal Serial Bus (USB) Function controller with eight flexible endpoint pipes, integrated transceiver, and 1KB FIFO RAM
 - d. Supply voltage regulator
 - e. True 10-bit 200 ksps differential / single-ended ADC with analog multiplexer
 - f. On-chip voltage reference and temperature sensor

- g.** On-chip voltage comparators (2)
- h.** Precision internal calibrated 12 MHz internal oscillator and 4x clock multiplier
- i.** Internal low-frequency oscillator for additional power savings
- j.** Up to 64 KB of on-chip Flash memory
- k.** Up to 4352 Bytes of on-chip RAM (256 + 4KB)
- l.** External memory interface (EMIF) available on 48-pin versions
- m.** SMBus / I2C, up to 2 UARTs, and Enhanced SPI serial interfaces implemented in hardware
- n.** Four general-purpose 16-bit timers
- o.** Programmable Counter / Timer Array (PCA) with five capture / compare modules and Watchdog Timer function
- p.** On-chip Power-On Reset, V_{DD} Monitor, and Missing Clock Detector
- q.** Up to 40 Port I/O (5V tolerant)

Apply to control the sensorless BLDC motor, the 10 bit ADC function is used to get Back-EMF and Speed-command. The PCA modules are used to generate PWM. Three Timers are used to clock and interrupt. Overall, the C8051F340 can deal with almost what the sensorless BLDC control needs.

4.2 Sensorless BLDC driver circuits

Fig 4.3 is the sensorless BLDC driver circuits. I divide the circuits into four parts. The first part is shown in Fig 4.4. Those circuits are used to display the data which I want to know. Examples of motor speed, commutation time, PWM and speed-command etc. The second part is shown in Fig 4.5. Those circuits are the MOSFET driver circuits. The C8051F340 microprocessor control unit sends PWM signals in the IC_DM74LS04N first. The IC makes two PWM signals invert. In other words, if the one signal is ON, another is OFF. They are complementary to each other. Then, the IC_DM74LS04N sends the complementary PWM signals in the IC_IR2110S. IC_IR2110S is the MOSFET driver. Through the driver, the PWM can drive the MOSFET successfully. The third part is shown in Fig 4.6. Those circuits are used to detect current which flow in the cement resistance. Use the differential amplifier to calculate the voltage across resistance. The fourth part is shown in Fig 4.7. This part is constructed of low pass filter. The goal is to filter the noise and get the Back-EMF. Fig 4.8 and Fig 4.9 are practical driver circuits. Fig 4.8 is the front view of the driver circuits and Fig 4.9 is the back view of the driver circuits.

4.3 Experiment results

The goal of the experiments is to compare sensor control with sensorless control. Fig 4.10 is my experiment instrument. The BLDC

motor connects to hysteresis dynamometer through shaft coupling. The hysteresis dynamometer adds loading to my BLDC motor step by step until my motor stalls, record the maximum torque, maximum current and efficiency at certain speed. Fig 4.11 is the maximum torque compare to motor speed. The sensorless control is worse than the sensor control under 1750 RPM. During 1750 RPM and 3750 RPM, the sensorless control is near to sensor control. Over 3750 RPM, the two control methods are very similar. Fig 4.12 is the current range of two control methods. Every bar has two sections at any speed. Lower section is the current range that the motor without loading in. Upper section is the current range that the motor has loading in. The current increases with the loading increase. The better current range which we want to control is also over 1750 RPM. Fig 4.13 is the comparison with mechanical power at different speed. The power increases with increasing speed. The maximum power is approximate to 3750 RPM with sensorless control. With sensor control, the maximum power is at 3500 RPM. Behind the maximum power, the power decreases with increasing speed. Fig 4.14 is the comparison with efficiency at different speeds. The speed is higher, the efficiency is higher. The efficiency of sensorless control is near to sensor control.

Chapter 5 Conclusion

Compare to general sensorless BLDC controls, I omit the Back-EMF detection circuits. Almost these propose that Back-EMF detection circuits replace hall sensors. The Back-EMF is detected by comparators and then estimate the commutation time. In an aspect of cost, just spend less money to Back-EMF detection circuits instead of much money to hall sensors. Remember! You still spend money for your Back-EMF detection circuits. In this thesis, I just ADC the voltage of excited phase to estimate the zero crossing point of the Back-EMF without any extra circuits or sensors. In other words, I don't pay any money on detecting Back-EMF. This is an advantage to using the method.

Of course, there are very restricts with the method. First, the motor must be moving at a minimum rate to generate sufficient Back-EMF to be sensed. Second, abrupt changes to the motor load can cause the Back-EMF drive loop going out of lock. Third, commutation at rates faster than the ideal rate will result in a discontinuous motor response. Fourth, as the results of the experiments, the torque is worse at lower speed.

Overall, if low cost is a primary concern and low speed motor operation is not a requirement and the motor load is not expected to change rapidly then sensorless control may be the better choice for your application.

Reference

- [1] K. Y. Cheng and Y. Y. Tzou, "Design of a sensorless Commutation IC for BLDC Motors," IEEE Transactions on Power Electronics, vol.18, no.6, pp.1365-1375, November 2003.
- [2] S. Ogasawara and H. Akagi, "An approach to position sensorless drive for brushless dc motors," IEEE Tran. Industry Applications, vol. 27, no. 5, pp.928-933, Sep. /Oct. 1991.
- [3] H.C. Chen, Y.C. Chang and C.K. Huang "Practical sensorless control for inverter-fed BDCM compressors" IET Electr. Power Appl, Vol. 1, No. 1, January 2007.
- [4] Dennis Nolan, Maxime Teissier, and David Swanson, "A Novel Microcontroller-Based Sensorless Brushless DC (BLDC) Motor Drive for automotive Fuel Pumps," IEEE transactions on industry applications, Vol. 39, NO. 6, November/December 2003
- [5] H.C. Chen and C.M. Liaw, "Sensorless control via intelligent commutation tuning for brushless DC motor," IEE Proc-Electr. Power Appl., Vol. 146, No. 6, November 1999.
- [6] D.H. Jung and I.J. Ha, "Low-cost sensorless control of brushless DC motors using frequency-independent phase shifter," IEEE Transactions

on Power Electronics, vol. 15, no.4, pp.744-752, July 2000

- [7] J. Shao, D. Nolan, and T. Hopkins, "Improved direct back EMF detection for sensorless brushless DC (BLDC) motor drives" in Proc. IEEE-APEC Conf., 2003, pp.300-305
- [8] Y.-S. Lai, F.-S. Shyu and Y.-H. Chang, "Novel Sensorless PWM-controlled BLDCM Drives without using Position and Current sensors, Filter and Center-Tap voltage" Industrial Electronics Society, The 29th Annual Conference of the IEEE, vol.3, pp. 2144-2149, Nov. 2-6 2003
- [9] 鄭光耀，無刷直流馬達無感測控制方法之研究與DSP實現技術之發展，國立交通大學電機與控制工程系，博士論文，2003
- [10] 程思穎，直流無刷馬達無感測驅動技術之實現，國立交通大學電機與控制工程系所，碩士論文，2005
- [11] 林翰宏，無刷直流馬達之分析與無感測器驅動之建模，國立交通大學電機與控制工程系所，碩士論文，2003

Table

Electrical angle	segment	Switch on
$0^\circ \sim 60^\circ$	$C\bar{B}$	S_3, S_5
$60^\circ \sim 120^\circ$	$A\bar{B}$	S_1, S_5
$120^\circ \sim 180^\circ$	$A\bar{C}$	S_1, S_6
$180^\circ \sim 240^\circ$	$B\bar{C}$	S_2, S_6
$240^\circ \sim 300^\circ$	$B\bar{A}$	S_1, S_4
$300^\circ \sim 360^\circ$	$C\bar{A}$	S_3, S_4

Table 2.1 The schedule of 120° six-step square commutation

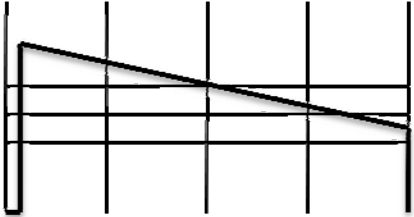
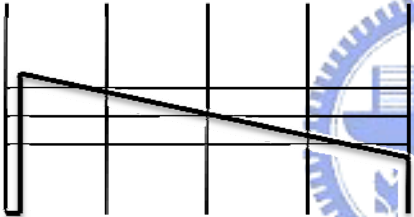
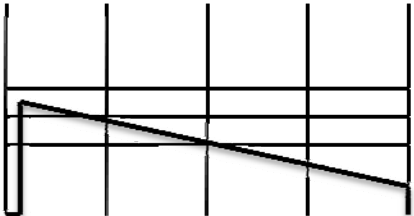
Waveform	Speed	Voltage
	Too fast	Too low
	Just right	Just right
	Too slow	Too high

Table 3.1 Back-EMF waveform control

Figure

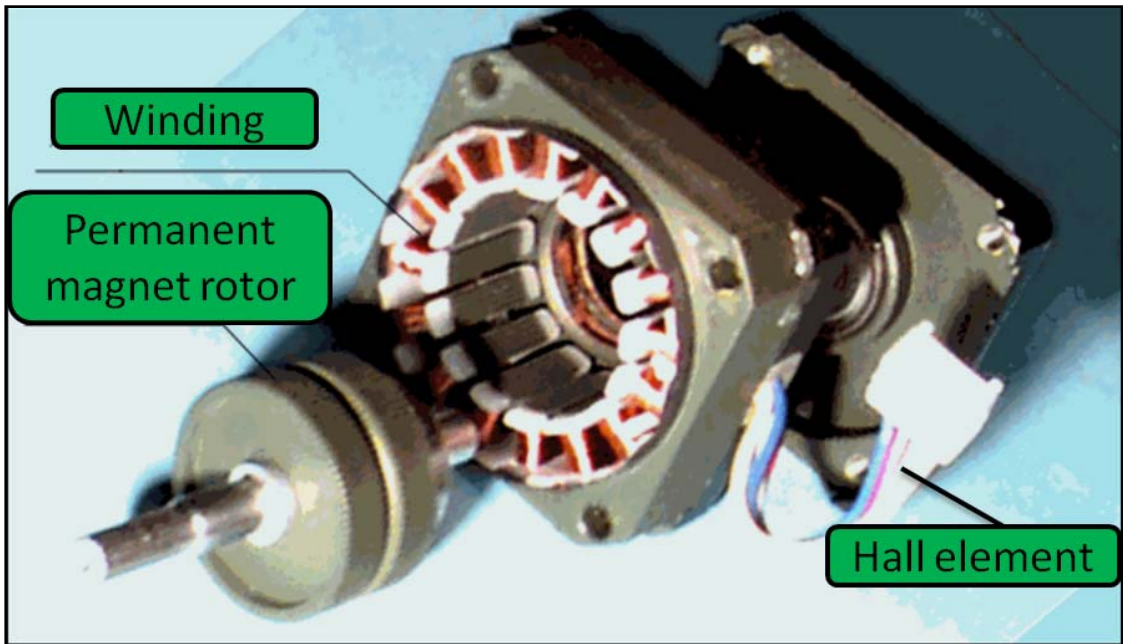


Fig 2.1 The configuration of BLDC motors

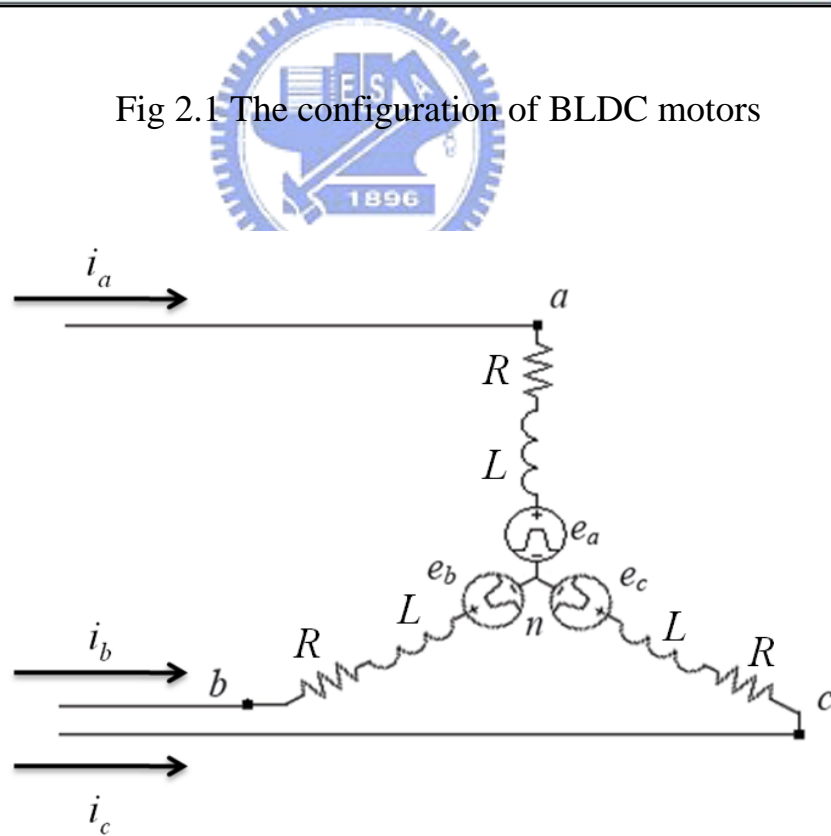


Fig 2.2 Equivalent modeling for a BLDC Motor

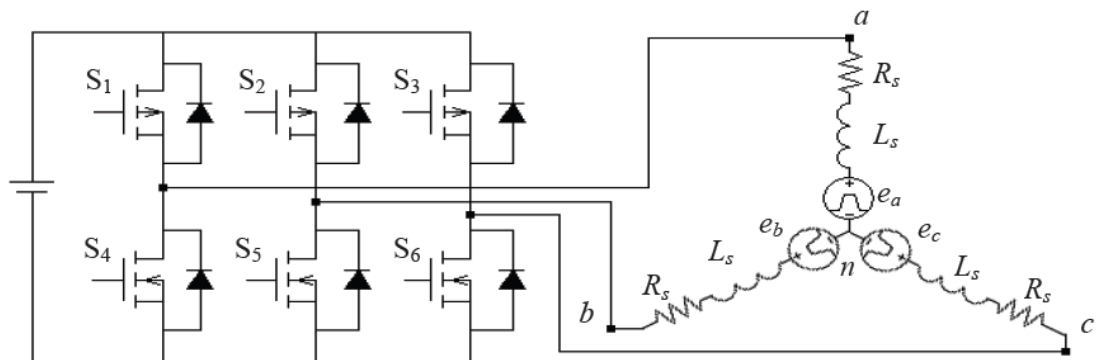


Fig 2.3 Schematic of the inverter and equivalent modeling for a BLDC motor

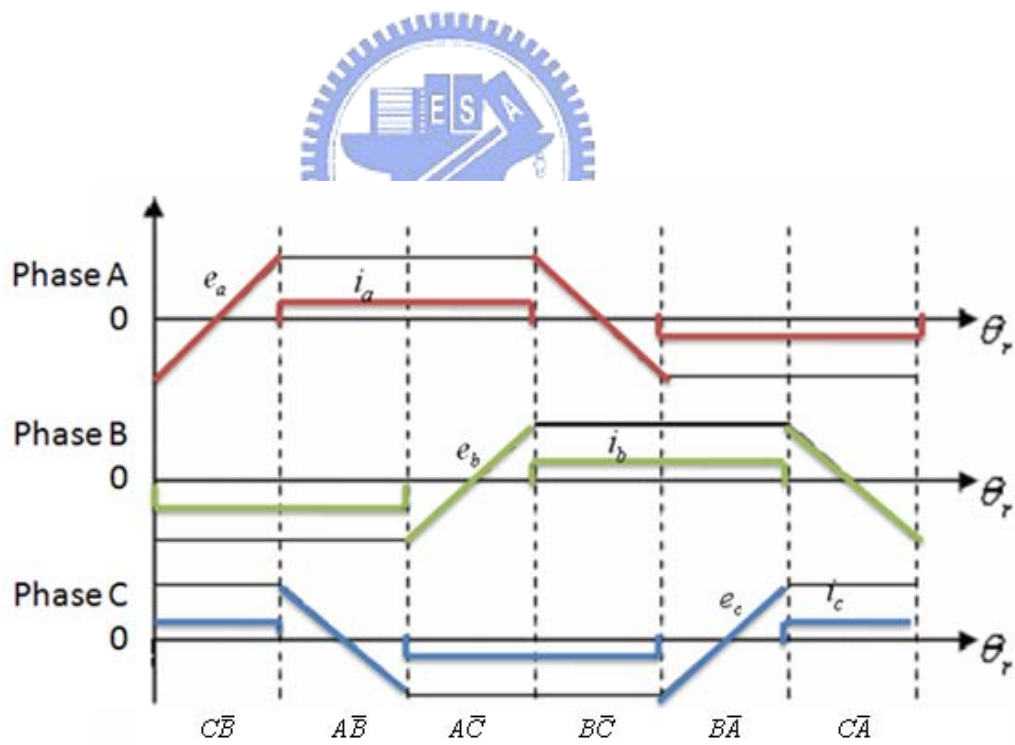


Fig 2.4 Ideal BEMF and phase current waveform of a BLDC motor

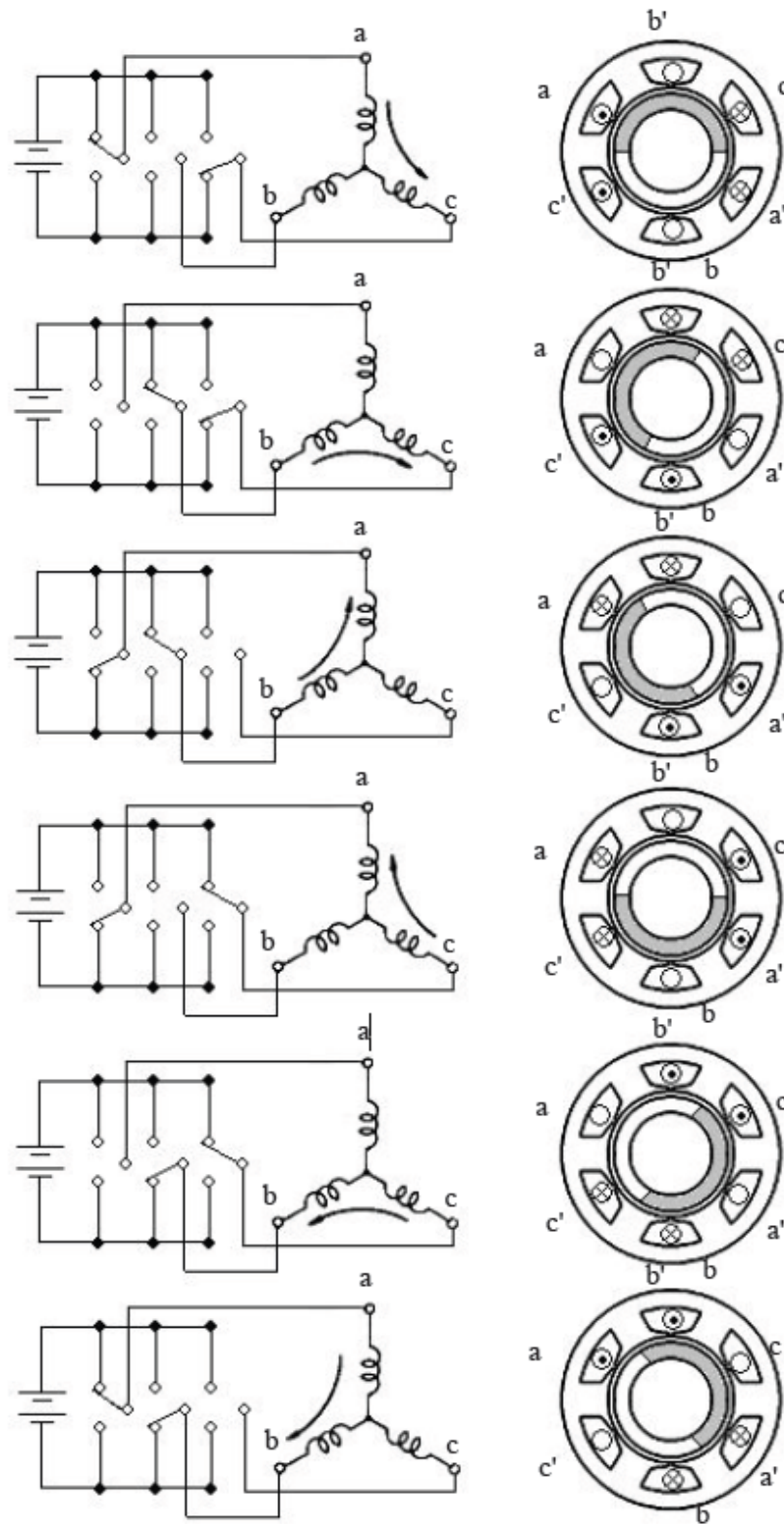


Fig 2.5 The procedure of six-step drive

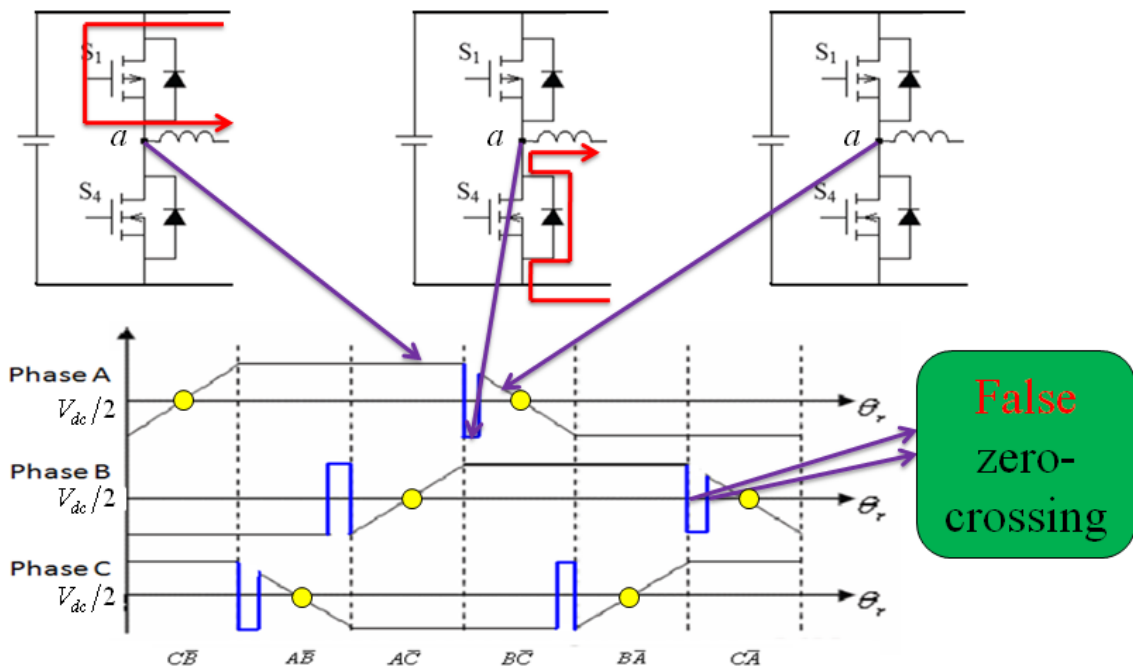


Fig 2.6 Phase voltage in commutation

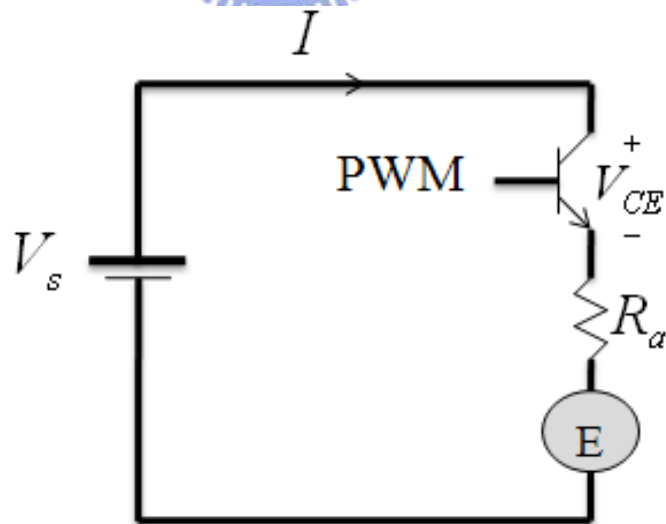


Fig 2.7 A BLDC motor equal circuits

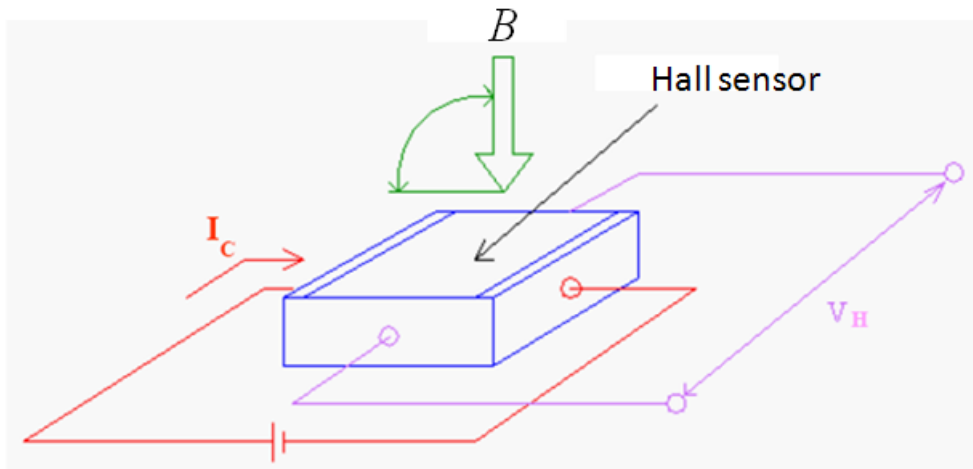


Fig 2.8 Hall-sensor

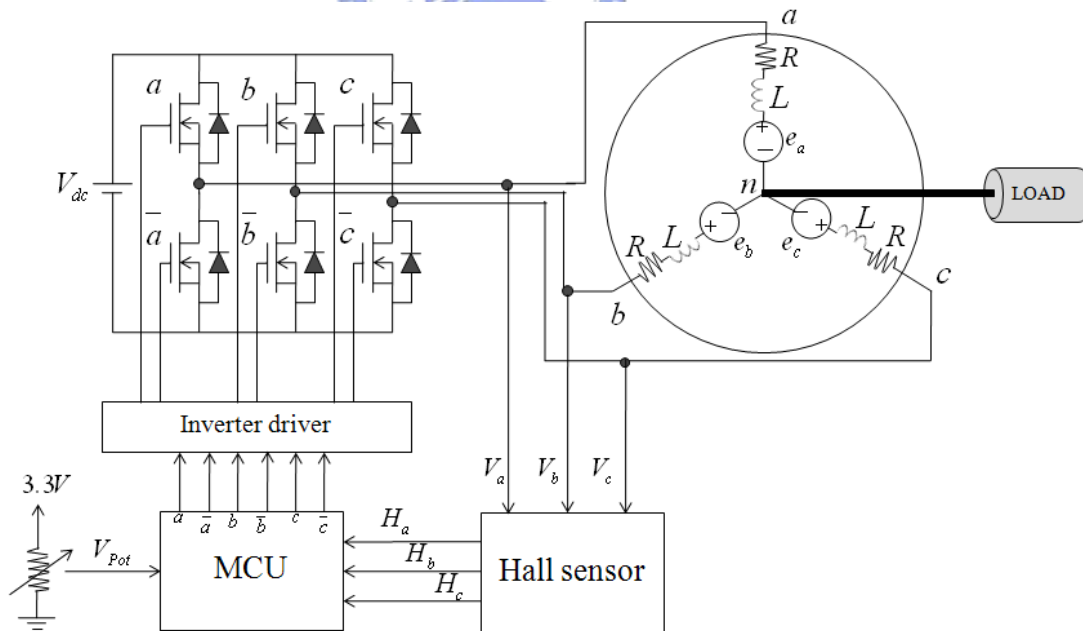


Fig 2.9 System framework of typical Hall-sensors commutation control

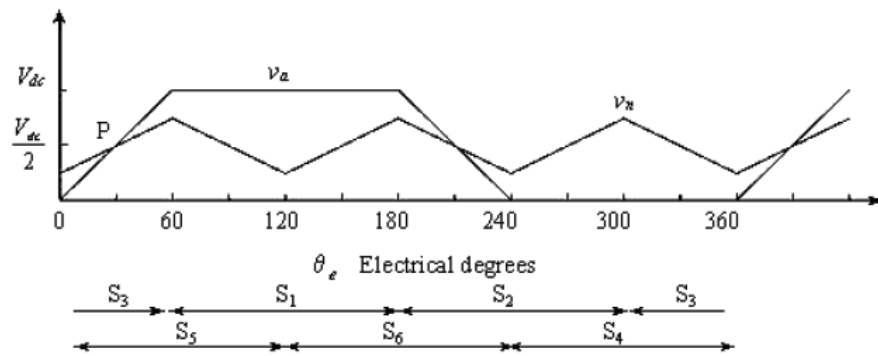


Fig 2.10 Detection of switching point P from the crossing of the neutral voltage and terminal voltage.

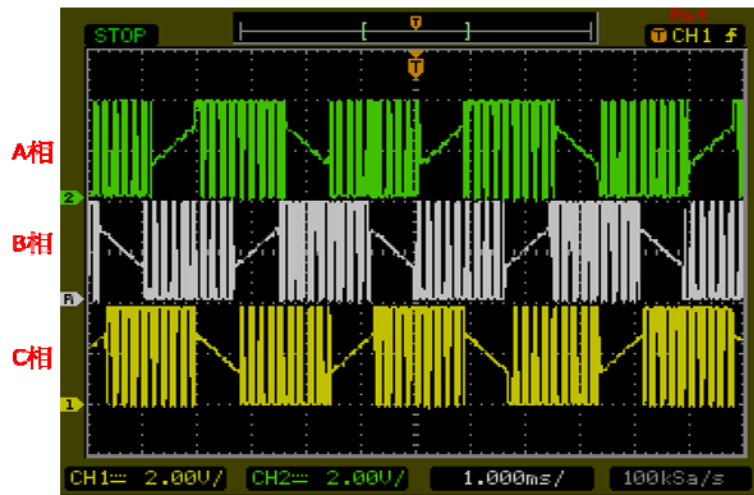


Fig 3.1 3-Phases voltage

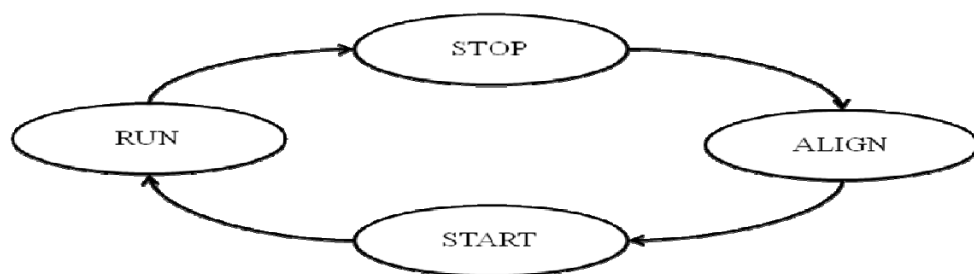


Fig 3.2 Sensorless BLDC state diagram

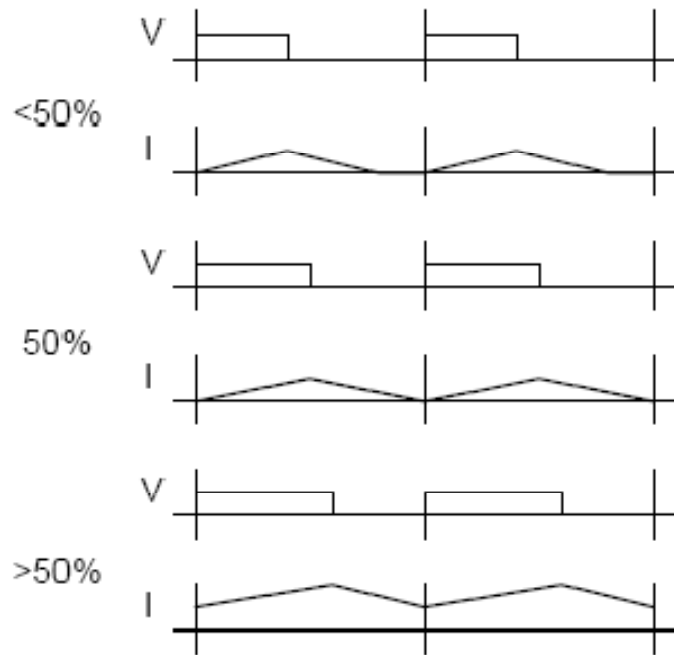


Fig 3.3 Motor current compare to duty cycle

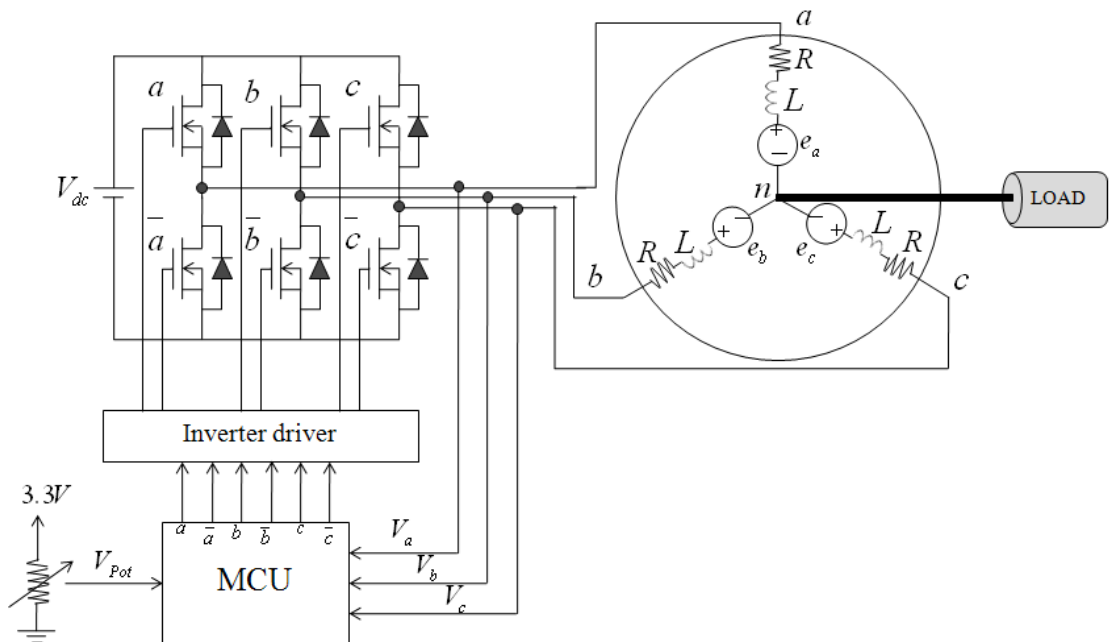


Fig 3.4 System frameowrk of sensorless cotrol

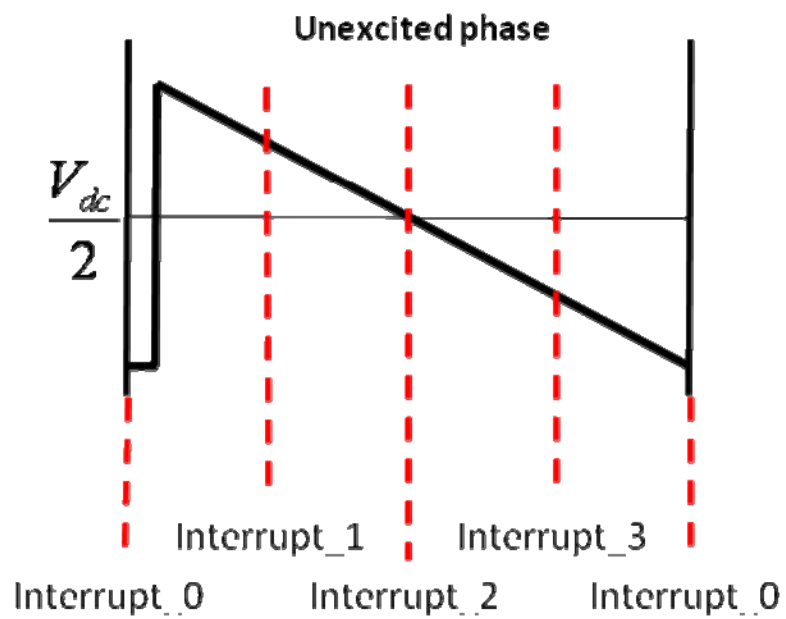


Fig 3.5 four slots in the unexcited phase

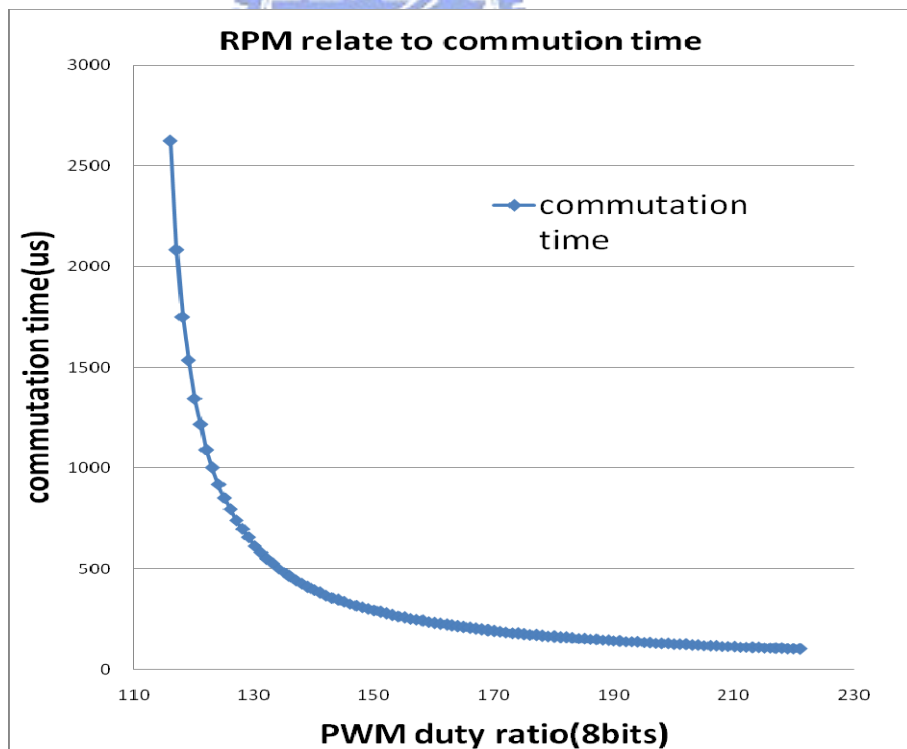


Fig 3.6 The relationship between PWM and commutation time without loading

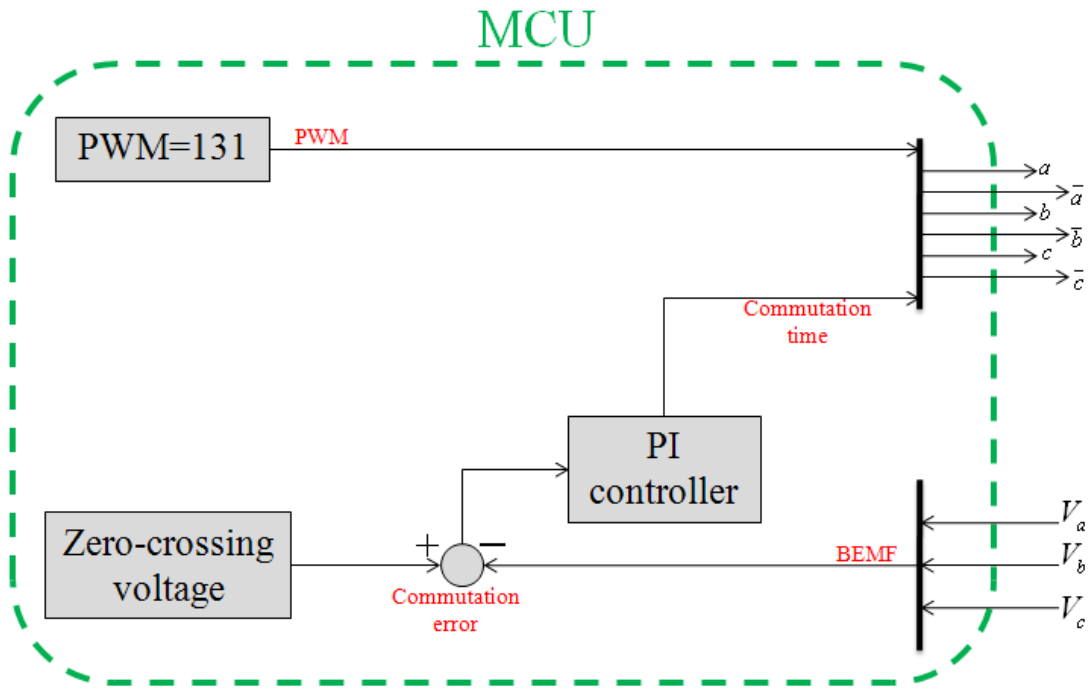


Fig 3.7 Synchronous mode function block of MCU

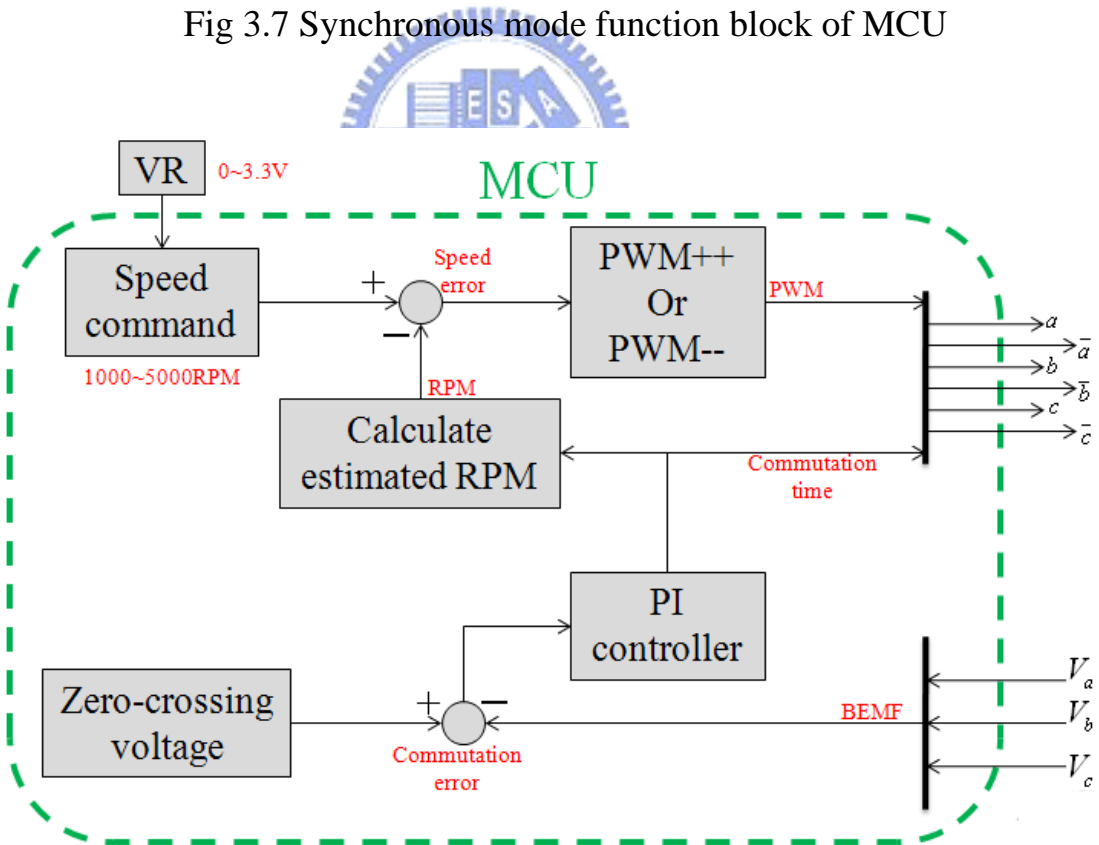


Fig 3.8 Accelerate mode function block of MCU

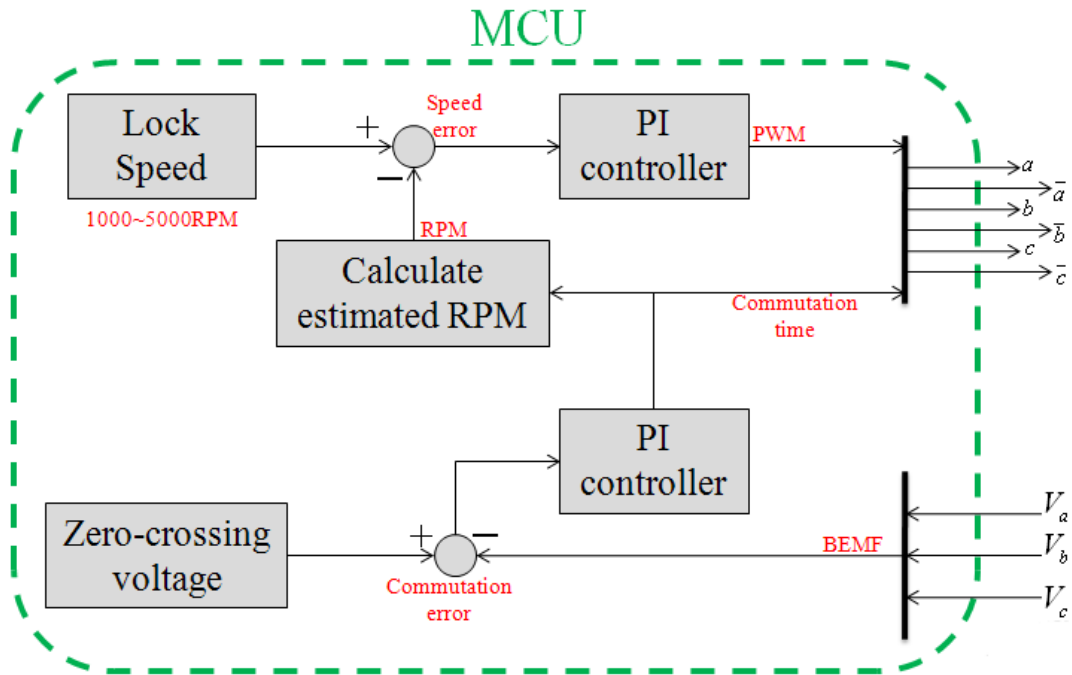


Fig 3.9 Speed locked mode function block of MCU

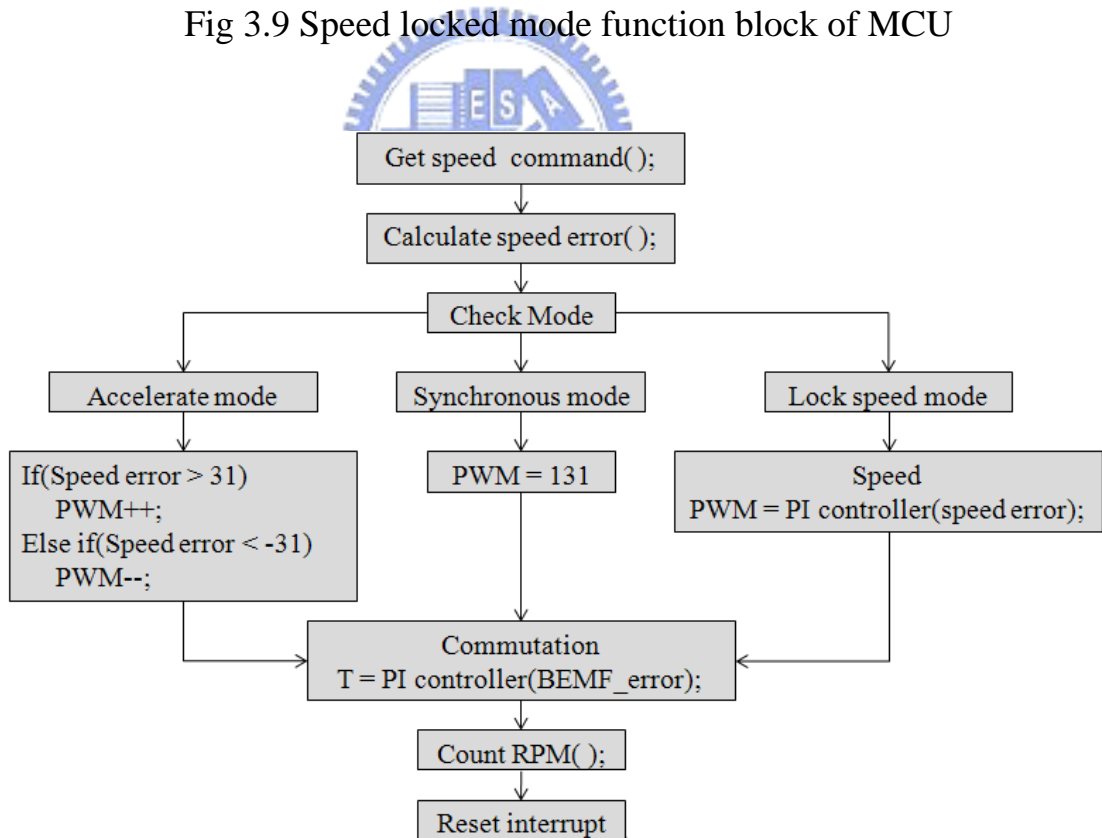


Fig 3.10 Flow char of feedback control

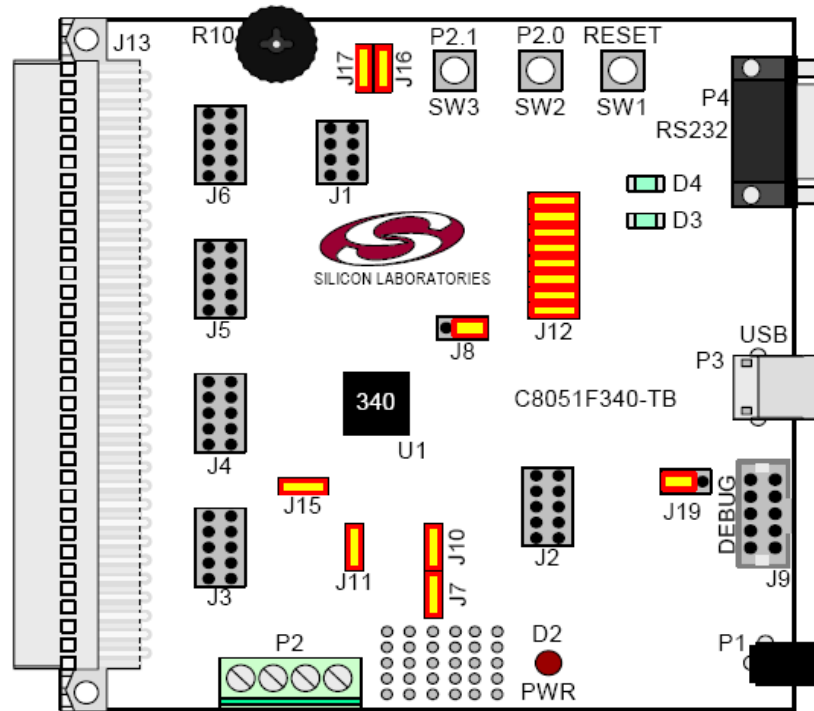


Fig 4.1 C8051F340 target board

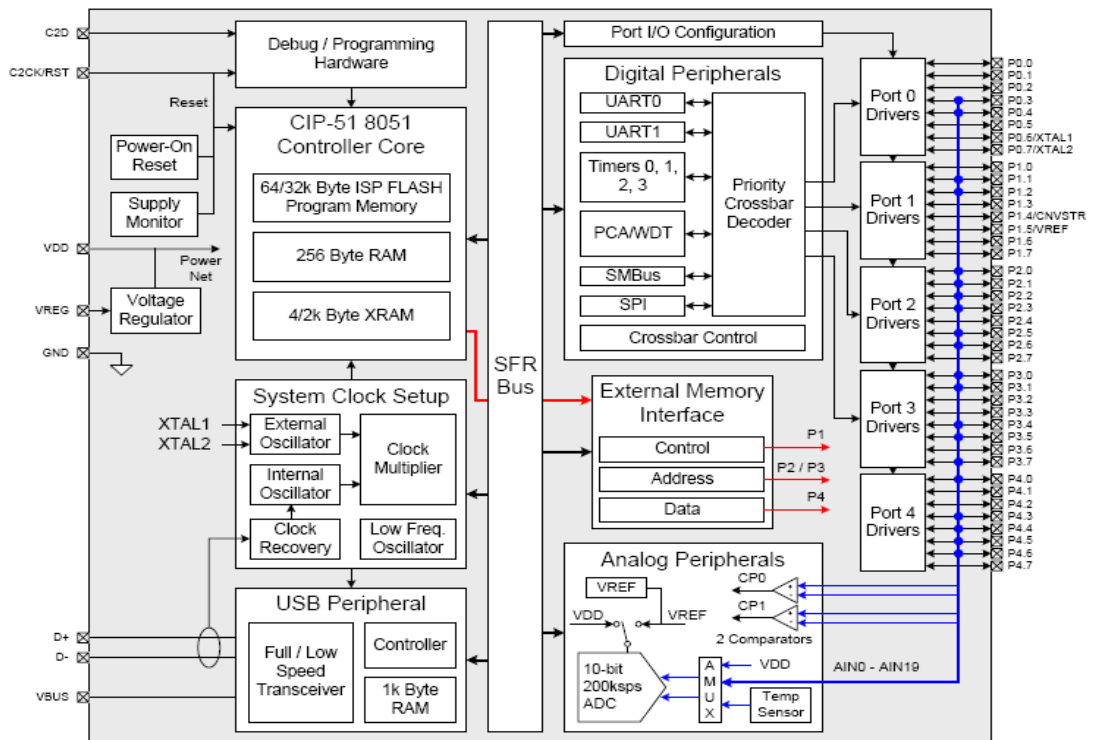


Fig 4.2 C8051F340 block diagram

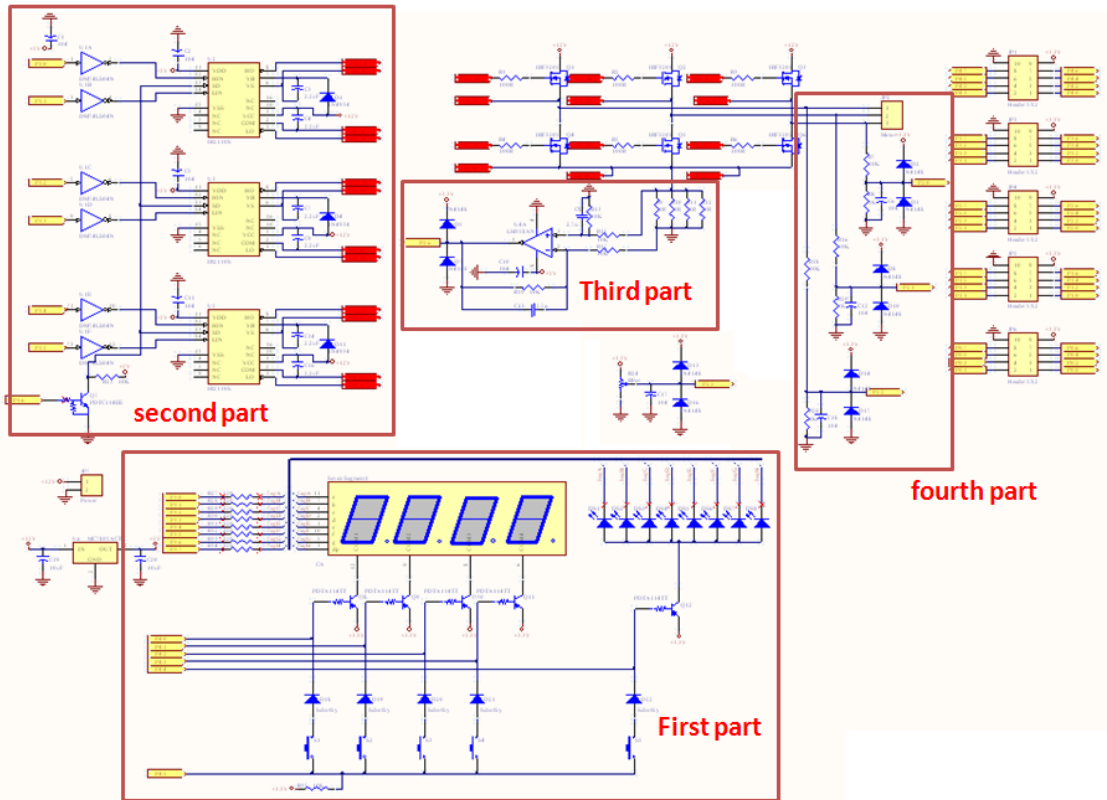


Fig 4.3 The sensorless BLDC driver circuits

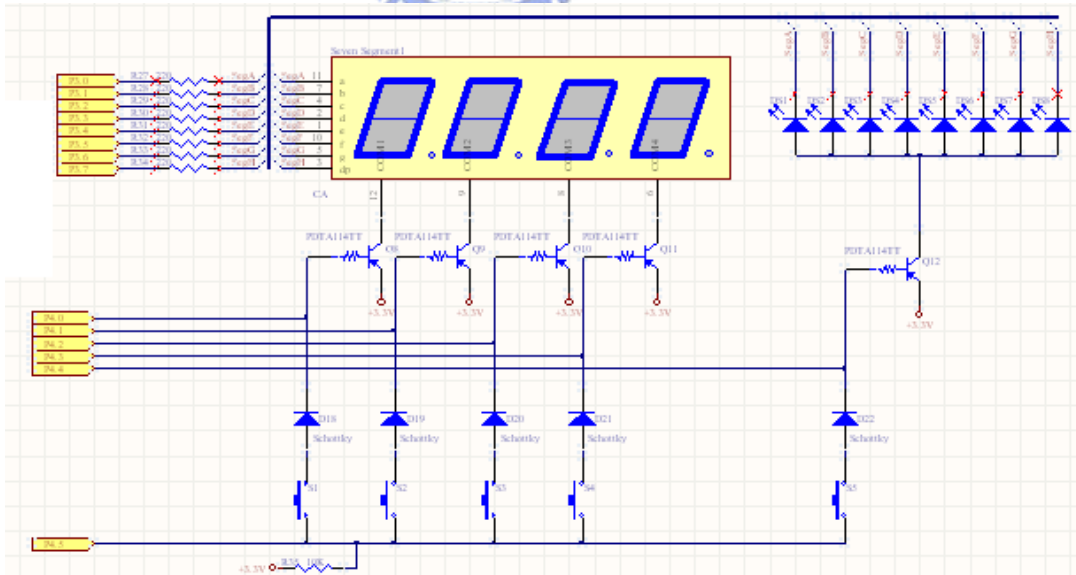


Fig 4.4 Display circuits

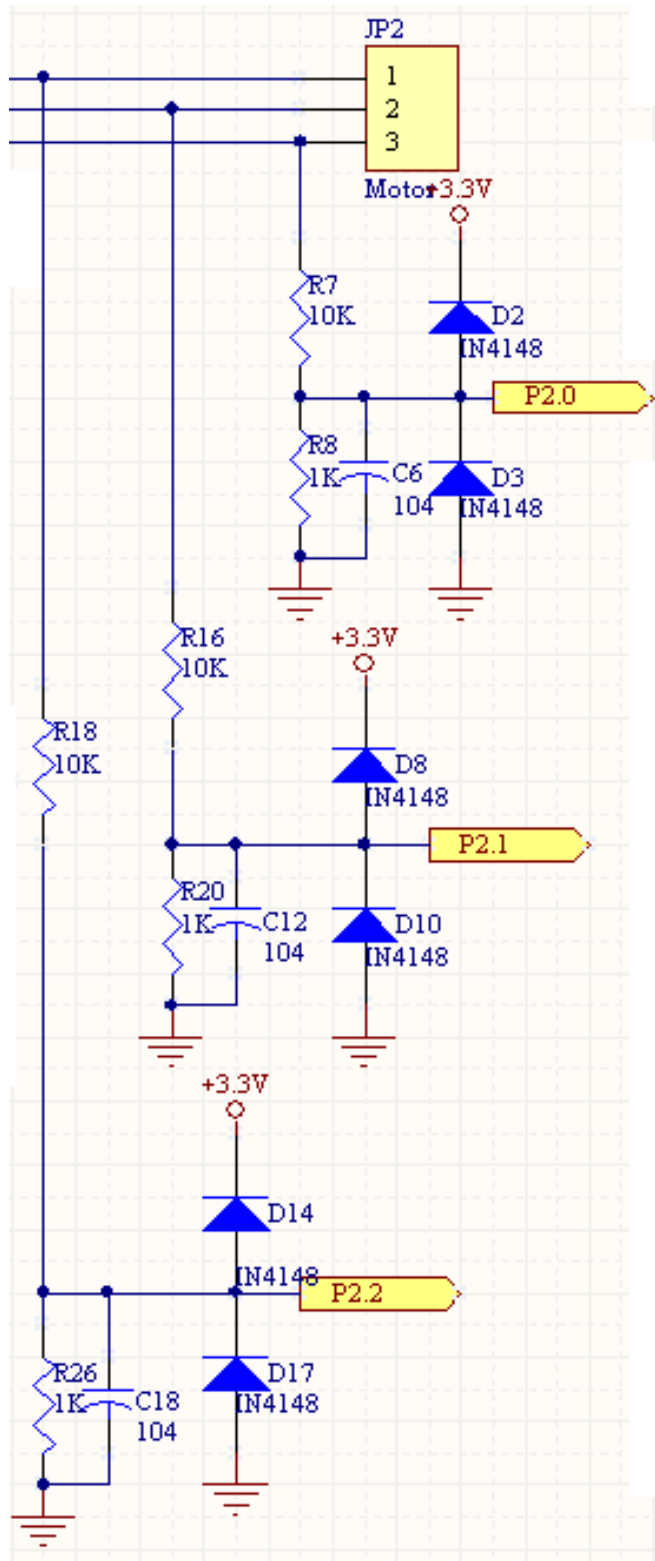


Fig 4.7 Lowpass filter circuits for filter noise

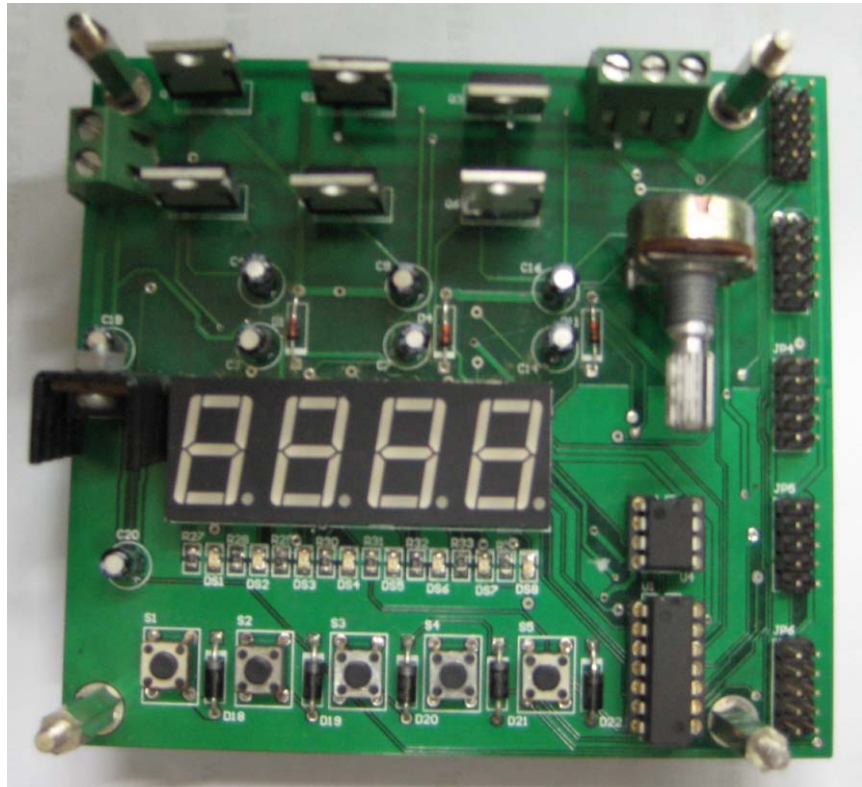


Fig 4.8 A front view of driver circuits

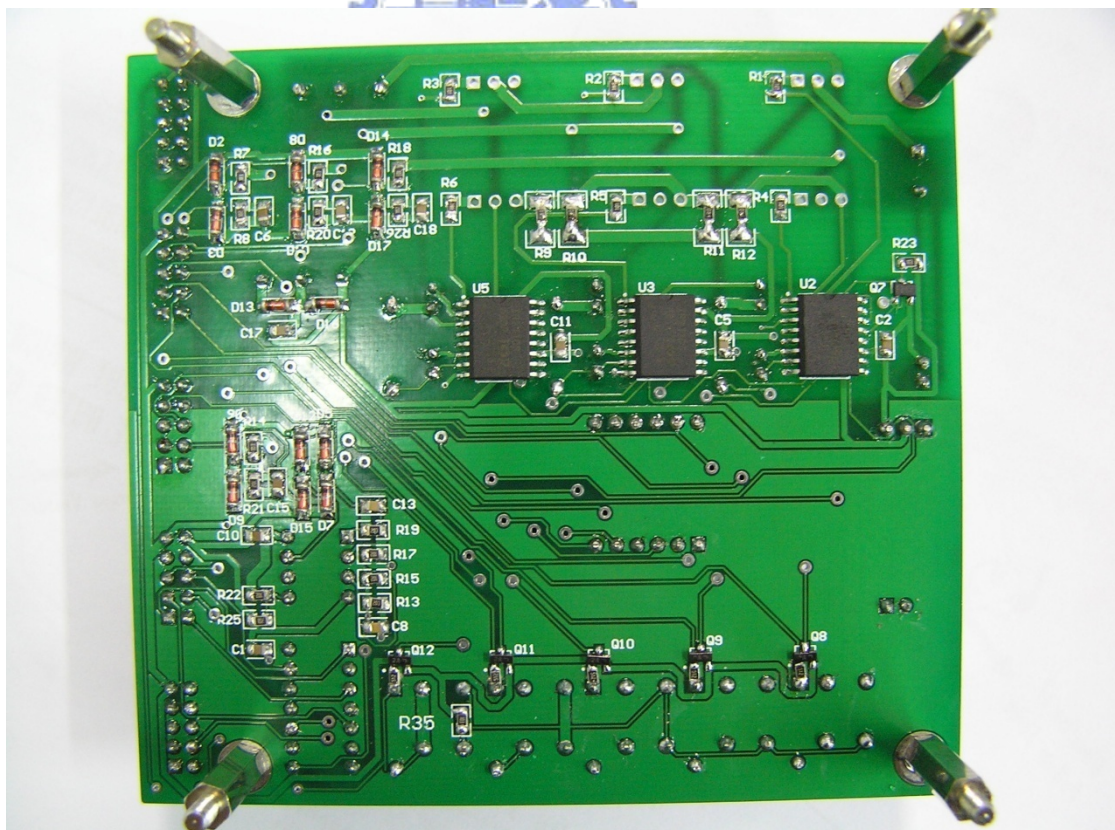


Fig 4.9 A back view of driver circuits

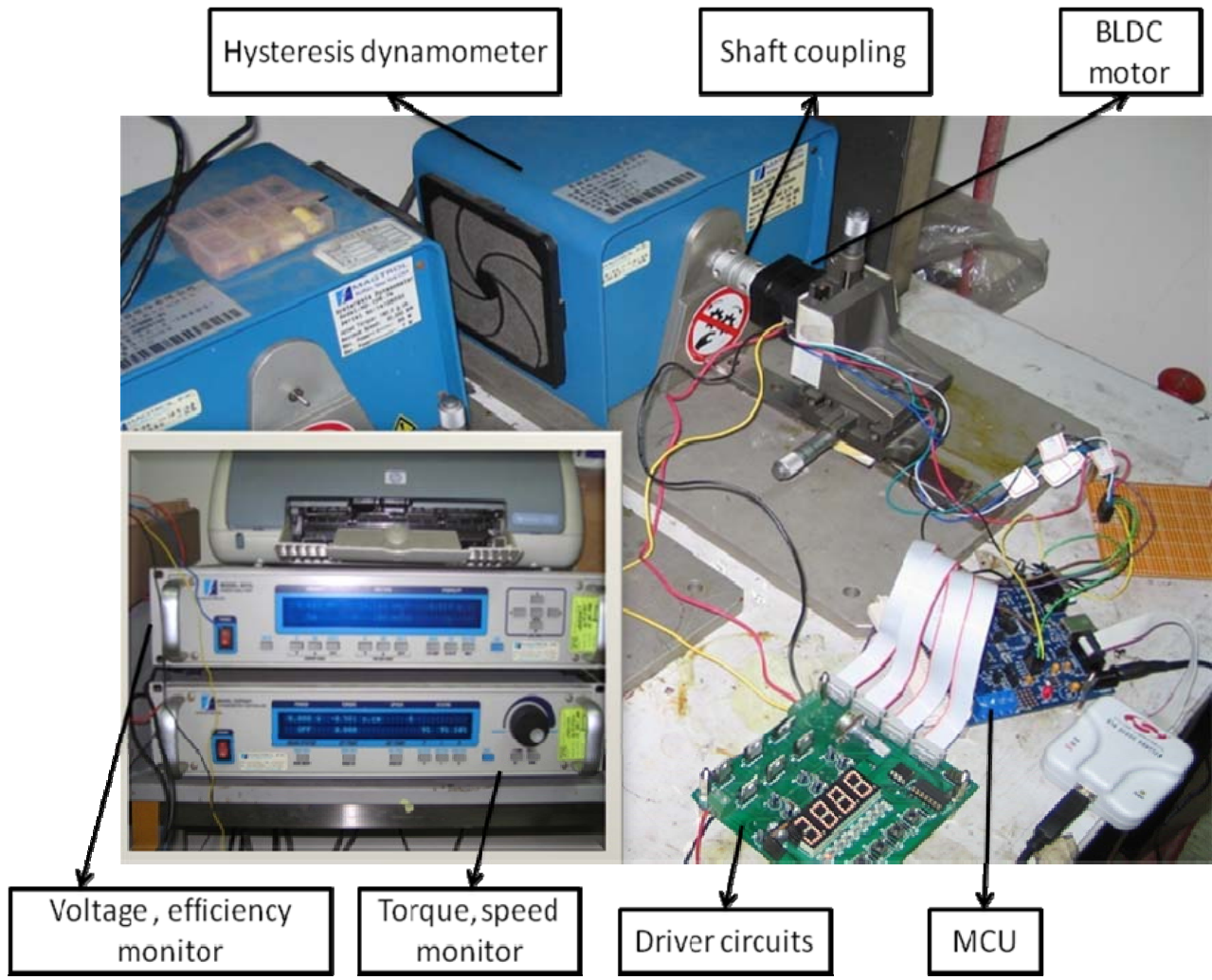


Fig 4.10 Experiment instrument

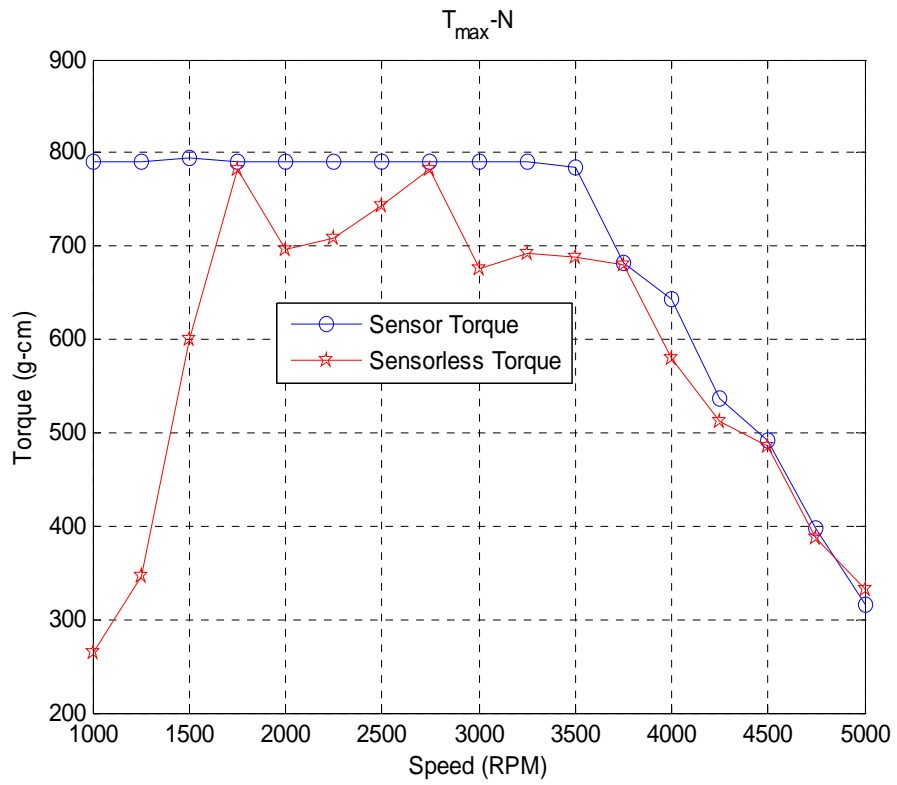


Fig 4.11 Maximum torque compares to motor speeds

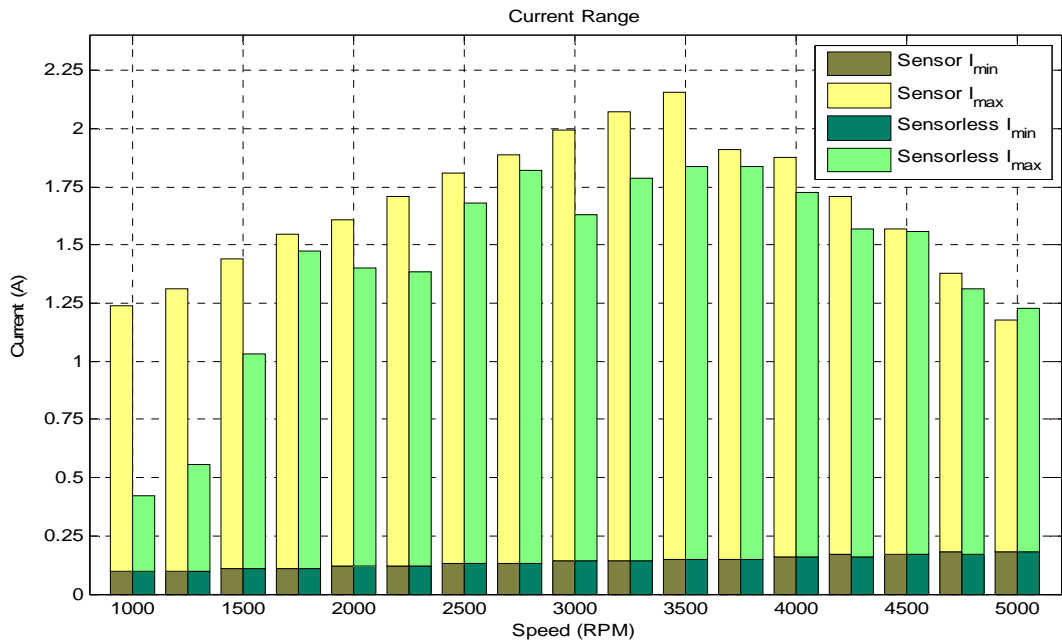


Fig 4.12 Current ranges compare to motor speeds

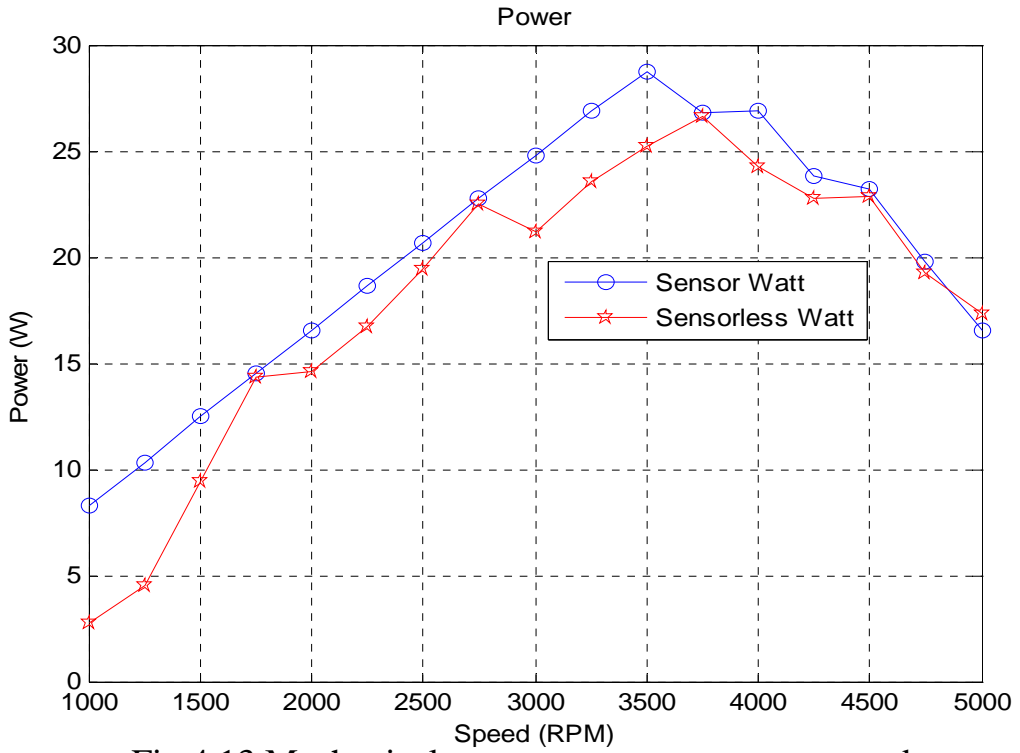


Fig 4.13 Mechanical power compare to motor speeds

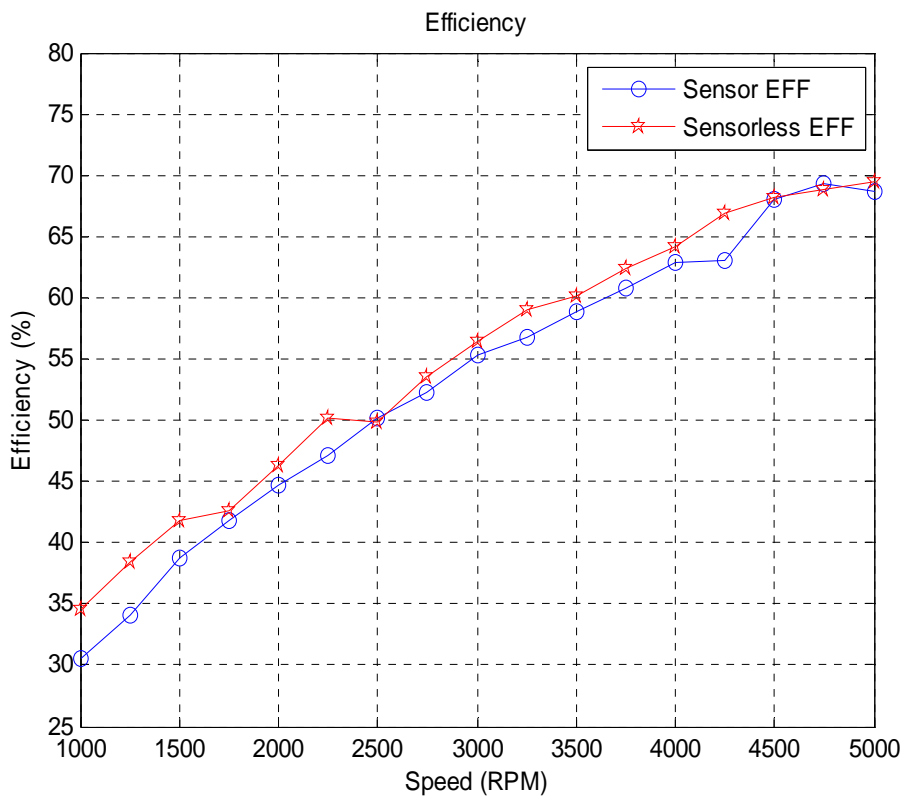


Fig 4.14 Efficiency compare to motor speeds